Analysing bifurcations encountered in numerical modelling of current transfer to cathodes of dc glow and arc discharges

2009 J. Phys. D: Appl. Phys. 42 194010

(http://iopscience.iop.org/0022-3727/42/19/194010)

IOP PUBLISHING JOURNAL OF PHYSICS D: APPLIED PHYSICS

J. Phys. D: Appl. Phys. **42** (2009) 194010 (21pp) doi:10.1088/0022-3727/42/19/194010

Analysing bifurcations encountered in numerical modelling of current transfer to cathodes of dc glow and arc discharges

P G C Almeida, M S Benilov, M D Cunha and M J Faria

Departamento de Física, Universidade da Madeira, Largo do Município, 9000 Funchal, Portugal

Received 11 April 2009, in final form 22 May 2009
Published 18 September 2009
Online at stacks.iop.org/JPhysD/42/194010

Abstract

Bifurcations and/or their consequences are frequently encountered in numerical modelling of current transfer to cathodes of gas discharges, also in apparently simple situations, and a failure to recognize and properly analyse a bifurcation may create difficulties in the modelling and hinder the understanding of numerical results and the underlying physics. This work is concerned with analysis of bifurcations that have been encountered in the modelling of steady-state current transfer to cathodes of glow and arc discharges. All basic types of steady-state bifurcations (fold, transcritical, pitchfork) have been identified and analysed. The analysis provides explanations to many results obtained in numerical modelling. In particular, it is shown that dramatic changes in patterns of current transfer to cathodes of both glow and arc discharges, described by numerical modelling, occur through perturbed transcritical bifurcations of first- and second-order contact. The analysis elucidates the reason why the mode of glow discharge associated with the falling section of the current–voltage characteristic in the solution of von Engel and Steenbeck seems not to appear in 2D numerical modelling and the subnormal and normal modes appear instead. A similar effect has been identified in numerical modelling of arc cathodes and explained.

(Some figures in this article are in colour only in the electronic version)

1. Introduction

Bifurcations of current transfer to cathodes of dc gas discharges or their consequences are sometimes encountered in apparently simple situations. As an example, figure 1 shows the current–voltage characteristics (CVCs) of a dc glow discharge calculated in the framework of a simple drift-diffusion model under different approximations: in one dimension (1D) without account of diffusion of the ions and the electrons; in 1D with account of (axial) diffusion; in two dimensions (2D) under the approximation of axial symmetry with account of diffusion both in the axial direction and to the (absorbing) wall.

The 1D solutions with and without diffusion are rather close to each other and represent in essence the classic solution of von Engel and Steenbeck (e.g. [1]). The physical meaning of this solution is well known: it describes the Townsend discharge at very low currents, the abnormal discharge at relatively high currents and a mode associated with the falling section of the CVC at intermediate currents, which is unstable and is not realized. The 2D solution is close to the 1D solution with account of diffusion at low and high currents; however, at intermediate currents it describes the subnormal and normal modes rather than the mode associated with the falling section of the CVC. Note that the ratio of the electron current to the wall of the discharge tube to the discharge current, evaluated with the use of the 2D solution, is of the order of 10^{-3} or lower at all discharge currents. In other words, diffusion of the charged particles to the wall is a weak effect and a question arises as to how this weak effect originates such a large difference, in particular, from where the subnormal and normal modes have appeared and where the mode associated with the falling section of the CVC has gone. These questions will be addressed in this work, and the identification and understanding of the relevant bifurcation are indispensable here.

As another example, figure 2 shows the CVC of the near-cathode region and temperatures T_c and T_e at the centre and edge, respectively, of the front surface of a cylindrical arc

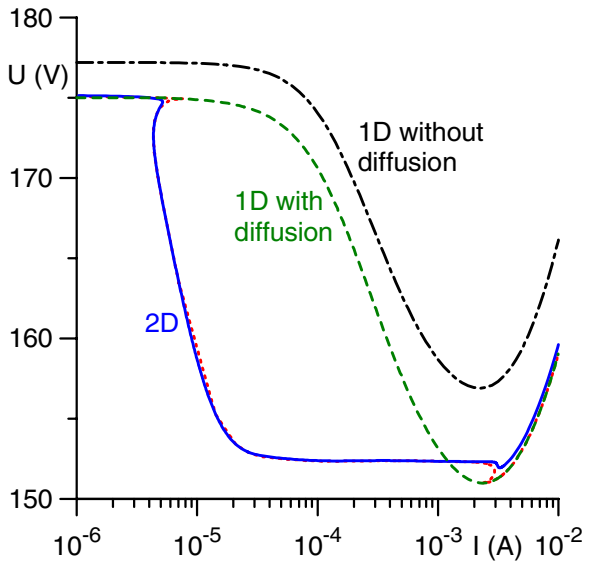

Figure 1. CVCs of the glow discharge: Xe plasma, $p = 30$ Torr, the discharge radius 1.5 mm and height 0.5 mm.

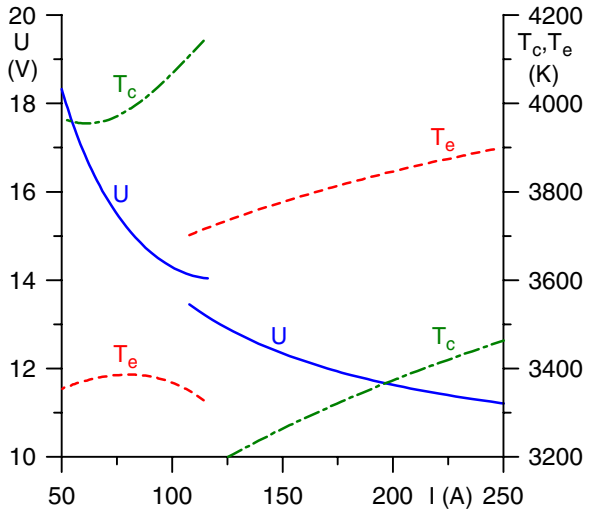

Figure 2. CVC of the near-cathode region of the arc discharge and temperatures at the centre and the edge of the front surface of the cathode. Simulation by means of the Internet tool [2] with the use of the built-in initial approximation. Ar plasma, $p = 1$ bar, W cathode of 2 mm radius and 10 mm height.

cathode, calculated by means of the Internet tool [2]. The code starts from a 1D initial approximation describing the diffuse mode on a cathode with an insulated lateral surface, and then gradually eliminates the insulation until a solution for a fully active lateral surface has been found. Under the conditions considered, this approach works nicely at the near-cathode voltages U below approximately 13.46 V. The obtained CVC $U(I)$ is falling and $T_c < T_e$; typical features of the diffuse mode of operation of an arc cathode. There is no convergence at U between 13.46 and 14.04 V. The convergence re-appears at $U \gtrsim 14.04$ V. The CVC remains falling, however $T_c > T_e$: it looks like a mode with a spot at the centre of the front surface of the cathode. Questions arise as to why simulations which start from the diffuse mode on a cathode with the insulating lateral surface are unable to arrive at the diffuse mode on a cathode with the active lateral surface and what significance the value $U = 13.46$ V has at which the troubles start. These questions also will be addressed in this work and will be shown to be related to the preceding ones.

The above examples show that a failure to recognize and properly analyse a bifurcation may create difficulties in numerical modelling and hinder understanding of numerical results and the underlying physics. In more general terms, the importance of understanding bifurcations of steady-state current transfer to cathodes of gas discharges may be explained as follows.

It has been known for many decades that dc glow discharges may operate in the abnormal mode or in the mode with a normal spot (e.g. [1]; some further references can be found in [3, 4]). Recently, also modes with regular patterns of two and more spots have been observed [5–10]. Different modes of current transfer to cathodes of high-pressure arc discharges have been observed since the early 1950s; e.g. [11–18]. A variety of different modes were reported, the most frequent being a diffuse mode and a constricted, or spot, mode.

An adequate theoretical description of multiple modes of current transfer to a dc discharge cathode does not necessarily involve essentially different physical mechanisms. Rather, this is a self-organization problem and as such it is intimately related to multiplicity of solutions: an adequate theoretical model of current transfer to a dc discharge cathode must in some cases allow multiple steady-state solutions to exist for the same conditions (in particular, for the same discharge current), different solutions describing different modes of current transfer.

Powerful solvers of non-linear multidimensional differential equations that exist nowadays can be used for finding multiple solutions in the same way as unique ones, provided, however, that one knows that multiple solutions do exist, where they should be sought and what they are like. Bifurcation analysis is a powerful means of obtaining such qualitative information. Of course, this qualitative information also facilitates analysis and understanding of the obtained numerical results and the underlying physics. One more reason to study bifurcations of current transfer to cathodes of dc gas discharges is their intimate relation to stability of different steady-state modes.

In order to illustrate the above statements, one can mention a few examples. A study of symmetry-breaking bifurcations, such as branching of 2D and 3D solutions from 1D solutions or of 3D solutions from 2D solutions, is probably the simplest way of proving existence of multiple solutions to nonlinear multidimensional differential equations and of establishing the pattern of these solutions including conditions of their existence, thus paving the way to finding these solutions numerically. In fact, this is how multiple solutions describing different modes of dc current transfer to both arc and glow cathodes have started to appear. Another example is represented by dramatic changes in patterns of dc current transfer that can occur in both glow and arc discharges, such as the variation of patterns in glow discharge caused by diffusion losses, which was mentioned above and is illustrated in figure 1, or the variations of patterns of steady-state modes of current transfer to arc cathodes under

conditions of industrial interest detected in [19, 20]. It will be shown in this work that these changes occur through perturbed transcritical bifurcations, and understanding these bifurcations indeed facilitates numerical modelling and analysis of its results. It will also be shown that ideas of the bifurcation theory provide useful information on the behaviour of different steady-state modes of current transfer in the vicinity of turning points.

This paper is concerned with analysis of bifurcations that have been encountered in numerical modelling of current transfer to cathodes of dc glow and arc discharges. In section 2, multiple solutions describing different modes of current transfer to cathodes of dc glow and arc discharges are briefly described and bifurcations that they exhibit are identified. Fold, transcritical and pitchfork bifurcations are analysed in sections 3, 4 and 5, respectively. The results obtained are discussed in section 6 and conclusions summarized in section 7. For convenience, a short summary of relevant information from the general bifurcation theory is given in appendix A.

2. Bifurcations of modes of current transfer to cathodes of dc discharges

In the course of the last decade, an approach to simulation of multiple modes of current transfer to dc discharge cathodes based on providing multiple solutions has become virtually universally accepted in the modelling of plasma–cathode interaction in high-pressure arc discharges. Multiple solutions describing different modes have been calculated by a number of authors [19–30] on the basis of the so-called model of non-linear surface heating and validated by an extensive comparison with the experiment; see review [31] and references therein. Self-consistent modelling of the diffuse and spot modes on arc cathodes of a given shape has become almost trivial; one can mention, as an example, a free Internet tool [2] for simulation of axially symmetric modes on cylindrical cathodes, which also computes bifurcation points and serves as a tutorial on finding multiple solutions describing diffuse and spot modes.

Multiple solutions in the theory of dc glow discharges have just started to appear [32, 33]. It was found that such solutions exist even in the most basic model of glow discharge, which takes into account drift and diffusion of the single ion species and the electrons, volume ionization and recombination, and secondary electron emission while neglecting the possible presence of multiple ion and neutral species with a complex chemistry and the non-locality of the electron energy distribution.

In this section, the above-mentioned numerical models are briefly described, relevant multiple solutions are given and the bifurcations encountered are identified. It should be stressed that this work is concerned with a particular aspect of the multiple solutions, namely, with bifurcations that they exhibit; the reader is referred to the above-cited papers for a detailed discussion of solutions on the whole and of their physical meaning.

2.1. Models and numerics

The calculation domain is the interelectrode gap in the case of glow discharge and the body of a thermionic cathode in the case of arc discharge, and is assumed to be a circular cylinder of radius R and height h (except in the case of an arc cathode treated in section 4.3 where it has a hemispherical tip).

The distribution of the ion and electron densities n_i and n_e and the electrostatic potential φ in the interelectrode gap in the case of a glow discharge is described by the simplest self-consistent model which comprises equations of conservation of a single ion species and the electrons written in the drift-diffusion approximation (e.g. [34]) with account of electron impact ionization and dissociative recombination, and the Poisson equation. Results reported in this work refer to a discharge in xenon under the pressure of 30 Torr, $R = 1.5\,\mathrm{mm}$ and $h = 0.5\,\mathrm{mm}$. The mobilities of Xe_2^+ ions and electrons in Xe were set equal to $2.2 \times 10^{-3}\,\mathrm{m^2\,V^{-1}\,s^{-1}}$ and $0.57\,\mathrm{m^2\,V^{-1}\,s^{-1}}$, respectively, in accordance with [35, 36]. Townsend's ionization coefficient was evaluated by means of equation (4.6) of [1]. The diffusion coefficients were evaluated by means of the Einstein relation with temperatures of the ions and electrons equal to 300 K and 1 eV, respectively. The coefficient of dissociative recombination of molecular ions Xe_2^+ was set equal to $2 \times 10^{-13}\,\mathrm{m^3\,s^{-1}}$ [37, 38].

The simulation of the interaction of high-pressure arc plasmas with thermionic cathodes is based on the model of non-linear surface heating; e.g. [31]. In the framework of this model, the distribution of the temperature T inside the cathode is found by solving the equation of heat conduction with a non-linear boundary condition that describes the energy exchange of the cathode with the adjacent plasma. Densities of the energy flux and the electric current to the cathode surface are treated as known functions of the local temperature and the near-cathode voltage drop U: $q = q(T, U)$ and $j = j(T, U)$. These functions are calculated in advance by means of solving equations describing the near-cathode plasma layer in a high-pressure plasma which are summarized in [39]. Results reported in this work refer to an arc in atmospheric-pressure argon with a tungsten cathode, $R = 2\,\mathrm{mm}$ and $h = 10\,\mathrm{mm}$. Data on thermal conductivity κ of tungsten have been taken from [40].

Let us introduce cylindrical coordinates (r, ϕ, z) with the axis z coinciding with the axis of the calculation domain and with the origin at the centre of the surface of the glow cathode or at the centre of the front surface of the arc cathode. In the case of glow discharge, the boundary conditions at $z = 0$ and $z = h$ are the conventional ones: at $z = 0$, i.e. at the cathode, the ion diffusion current is neglected, the electron current is due to secondary emission (the effective secondary emission coefficient was set equal to 0.03) and the electrostatic potential vanishes; at $z = h$, i.e. at the anode, the electron diffusion current is neglected, the ion density vanishes and the electrostatic potential equals the discharge voltage U. In the case of the arc cathode, the front surface of the cathode, $z = 0$, is heated by the adjacent plasma and the boundary condition is $\kappa \frac{\partial T}{\partial z} = -q(T, U)$. The temperature at $z = h$, i.e. at the cathode base, is governed by the cooling arrangement and was set equal to 293 K.

In the case of glow discharge, one boundary condition at $r = R$, i.e. at the wall of the discharge tube, is zero density of electric current. The boundary conditions at $r = R$ for n_i and n_e are written in the form

$$s\, n_{i,e} + (1 - s)\frac{\partial\, n_{i,e}}{\partial\, r} = 0, \tag{1}$$

where s is a given parameter that varies between 0 and 1. $s = 0$ corresponds to a (totally) reflecting wall, or, in other words, to losses of the charged particles due to their diffusion to the wall being neglected. $s = 1$ corresponds to an absorbing wall, or, in other words, to diffusion losses being taken into account. In the case of the arc cathode, the boundary condition at $r = R$, i.e. at the lateral surface of the cathode, is written as

$$\kappa\frac{\partial T}{\partial r} = s\, q(T, U), \tag{2}$$

where s again is a given parameter varying between 0 and 1. $s = 0$ corresponds to the lateral surface of the cathode being thermally (and electrically) insulated, $s = 1$ corresponds to the lateral surface being active, i.e. energy- and current-collecting.

In the case of the arc cathode, the discharge current is related to T and U by the formula

$$I = \int j(T, U)\, \mathrm{d}S. \tag{3}$$

The integral here is evaluated over the front and lateral surfaces of the cathode, the contribution of the lateral surface being multiplied by s.

A natural control parameter for the calculation of steady-state solutions is the voltage U, which is defined as the discharge voltage in the case of glow discharge and as the voltage drop in the near-cathode plasma layer in the case of the arc cathode. However, this parameter is clearly inappropriate in the vicinity of extreme points of the CVC $U(I)$ of the mode being computed. Another possible control parameter is the discharge current I; however, it is inappropriate in the vicinity of turning points. Therefore, it is convenient to switch the control parameter while calculating steady-state modes. This can be achieved, e.g. by introducing an equation of external circuit with an appropriate variation of external resistance (ballast) and electromotive force along the mode being computed, or simply by switching between U and I as appropriate.

The situation turns different as far as bifurcations and stability are concerned: for example, an extreme point of the CVC $U(I)$ of a given mode, while being a regular point if the control parameter is I, becomes a turning point if the control parameter is U; conditions of stability of current- and voltage-controlled dc gas discharges are not the same. Since power supplies for gas discharges usually operate as current sources, bifurcations and stability will be discussed in this work under the assumption that the discharge is current-controlled.

The above-stated problems admit axially symmetric (2D) solutions, $f = f(r, z)$, 3D solutions, $f = f(r, \phi, z)$, and, in the particular case $s = 0$, also 1D solutions, $f = f(z)$. Here f designates the set of quantities n_i, n_e, φ in the case of glow discharge and T in the case of arc cathode. In this work, 1D and 2D steady-state solutions for the glow discharge and 1D, 2D and 3D solutions for the arc cathode are considered. Solutions for the glow discharge and 3D solutions for the arc cathode were calculated with the use of the commercial finite element software COMSOL Multiphysics. 1D and 2D solutions for the arc discharge were calculated with the use of the tool [2] except in the case of an arc cathode with a hemispherical tip, treated in section 4.3, where COMSOL Multiphysics was employed.

The above-stated problems possess axial symmetry, i.e. are invariant with respect to the transformation of rotation $\phi \to \phi + \alpha$, where α is any constant (a rotation angle). Therefore, if any of these problems admits a solution $f = f(r, \phi, z)$, then $f = f(r, \phi + \alpha, z)$ is a solution as well. In other words, each 3D solution represents an element of a continuum of 3D solutions that exist for the same discharge current and are identical to the accuracy of a rotation. An additional condition is required in order to single out one solution from this continuum, otherwise the problem will be ill-stated and iterations will not converge. 3D solutions reported in this work have been obtained in the following way [26, 28]: the calculation domain was restricted to half of the cathode, say, $0 \leqslant \phi \leqslant \pi$, and the symmetry condition $\partial T/\partial\phi = 0$ was imposed at the plane $\{\phi = 0, \phi = \pi\}$. Of course, this approach allows one to find only solutions that possess planar symmetry. We will come back to this point at the end of section 6.

Data on points of transcritical and pitchfork bifurcations of steady-state solutions reported in this work were obtained as follows. In the case of glow discharge, one of the bifurcating solutions is 1D and the other is 2D (these bifurcations will be designated $\{1D, 2D\}$ from now on) and the bifurcation points were found by means of solving the appropriate eigenvalue problem with the use of COMSOL Multiphysics. In the case of arc cathode, bifurcations $\{1D, 2D\}$, $\{1D, 3D\}$, $\{2D, 2D\}$, $\{2D, 3D\}$ and $\{3D, 3D\}$ are present. Points of bifurcations $\{1D, 2D\}$, $\{1D, 3D\}$ and $\{2D, 3D\}$ were calculated with the use of the tool [2], points of bifurcations $\{2D, 2D\}$ and $\{3D, 3D\}$ were calculated with the use of COMSOL Multiphysics. We note right now that calculated positions of bifurcation points in all the cases are in good agreement with the results of numerical calculations of steady-state solutions, as evidenced by the graphs that will follow.

Data on stability of current transfer to arc cathodes reported in this work were obtained by means of solving the appropriate eigenvalue problem with the use of COMSOL Multiphysics as described in [20].

2.2. Multiple solutions describing different modes of current transfer

An appropriate way to analyse multiple steady-state solutions is to start with the limiting case $s = 0$ (the case of the reflecting wall of the glow discharge tube or of insulating lateral surface of the arc cathode), where the pattern of solutions is the easiest to understand. CVCs for this case are shown in figures 3 and 4. Squares and circles in these and the following figures in the main body of the paper represent turning points and all the other bifurcation points, respectively. Also shown in

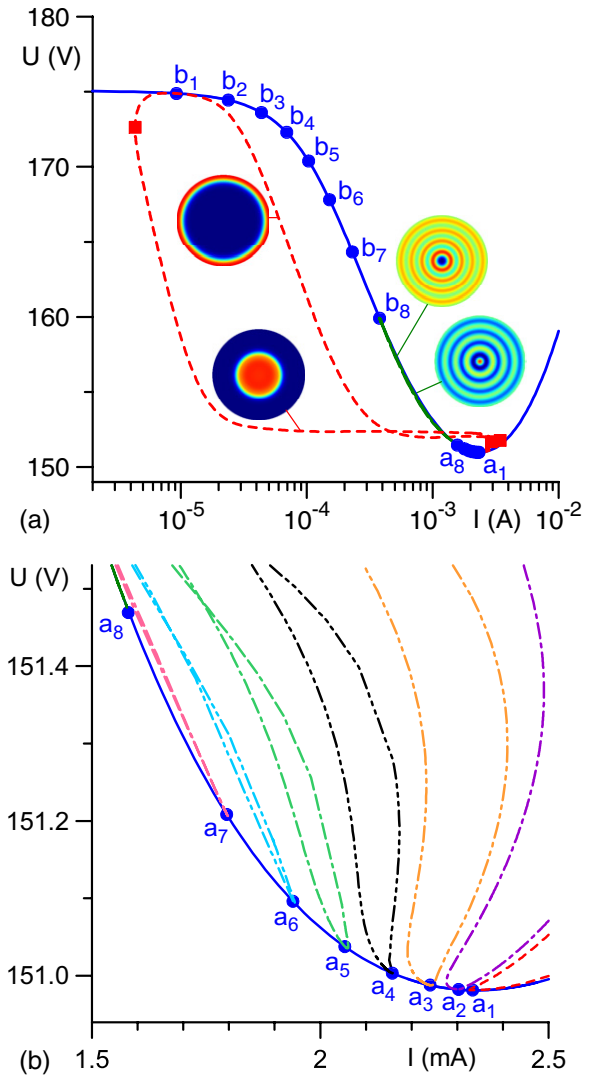

Figure 3. CVCs of different modes of current transfer in glow discharge with reflecting walls and schematics of current density distribution over the cathode surface. (*a*) The diffuse mode and the first and eighth 2D spot modes. The CVC of the eighth 2D spot mode coincides, to the graphical accuracy, with the CVC of the diffuse mode, also in (*b*). (*b*) CVCs in the vicinity of the point of minimum of the CVC of the diffuse mode.

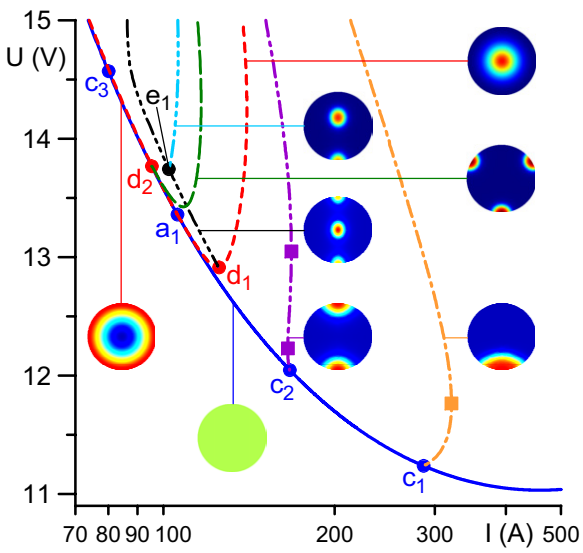

Figure 4. CVCs of steady-state modes of current transfer to arc cathode with insulating lateral surface and schematics of current density distribution over the front surface of the cathode.

figures 3 and 4 are schematics of distributions of current density over the cathode surface associated with each solution. (In the case of the arc cathode, only distributions along the front surface are shown.) The solid line in each figure represents the 1D solution, which describes a mode of current transfer with a uniform distribution of discharge parameters along the cathode surface. In the case of glow discharge, the 1D solution is the same as the one depicted by the dashed line in figure 1 and represents in essence the von Engel and Steenbeck solution. In the theory of the arc cathodes, the mode with a uniform distribution of discharge parameters along the current-collecting surface of the cathode is called diffuse. In the following, the mode described by the 1D solution will be called diffuse mode in the cases of both arc cathode and glow discharge.

There are also a number of 2D and 3D solutions describing different spot modes. While the diffuse mode exists at all currents, each of the spot modes exists in a limited current range.

In the case of glow discharge, eight 2D spot modes were detected. Let us number these modes in the order of shrinking of the range of currents in which they exist. The first and the eighth modes, i.e. those with the widest and narrowest ranges of existence, respectively, are shown in figure 3(*a*). Each mode joins the diffuse mode at two bifurcation points, one of these points being designated a_i and positioned in the vicinity of the point of minimum of the CVC of the diffuse mode, at $1.5 \lesssim I \lesssim 2.5$ mA (figures 3(*a*) and (*b*)) and the other, b_i, at low currents, $I \lesssim 0.4$ mA (figure 3(*a*)); here $i = 1, 2, \ldots, 8$. Let us number bifurcation points a_i from high to low currents, as shown in figure 3(*b*), and b_i from low to high currents, as shown in figure 3(*a*). A 2D spot mode which branches off from the diffuse mode at a bifurcation point a_i (or b_i) re-joins the diffuse mode at the bifurcation point b_i (or a_i, respectively) with the same number i. In the following, values of discharge current that correspond to the bifurcation points a_i and b_i will be designated $I(a_i)$ and $I(b_i)$, respectively.

The bifurcation points divide each 2D spot mode into two branches, one associated with a pattern consisting of a spot at the centre and possibly concentric ring spots, and the other associated with a pattern consisting of concentric ring spots without a spot at the centre. The number of inside ring spots (i.e. the number of maxima of the current density inside the interval $0 < r < R$) associated with an ith mode is $(i-1)/2$ if i is odd. If i is even, the number of inside ring spots is $i/2-1$ on the branch with a central spot and $i/2$ on the branch without a central spot. There is also a ring spot on the periphery of the cathode (i.e. there is a maximum of the current density at $r = R$) on the branch with or, respectively, without a central spot depending on whether i is even or odd.

In the case of the arc cathode depicted in figure 4, some spot modes join the diffuse mode and some do not. The mode that branches off from the diffuse mode at the bifurcation point

a_1 is 2D. The CVC of this mode is depicted by the short-dashed line and partially coincides with the CVC of the diffuse mode. This mode represents an analogue of the first 2D spot mode in the case of glow discharge and comprises two branches separated by the bifurcation point, one associated with a spot at the centre of the front surface of the cathode and the other with a ring spot on the periphery. Families of 3D modes with one spot on the periphery, or two spots on the periphery opposite each other, or three symmetrically positioned spots on the periphery branch off from the diffuse mode at the bifurcation points c_1, c_2 and c_3, respectively; the family of modes with three spots that branches off at the point c_3 is not shown in order not to overload the figure.

Comparing figures 3 and 4, one can say that the current and voltage range shown in figure 4 represents the vicinity of the point of minimum of the CVC of the diffuse mode. In other words, the spot modes in the case of the arc cathode branch off from the diffuse mode in the vicinity of the point of minimum, similarly to how it happens in the case of glow discharge. The question arises whether they re-join the diffuse mode at low currents. The range of currents down to 0.3 A (voltages of up to 1 kV) was investigated in order to answer this question. No re-joining was found; rather branching of two new families of 3D spot modes was detected: modes with four spots at the periphery, then modes with a spot at the periphery and an inside spot positioned opposite each other.

The three-dot-dashed line in figure 4 represents a family of 3D modes with a spot at the centre and two spots on the periphery positioned opposite each other, which branches off from the first 2D spot mode at the bifurcation point d_1. Note that patterns associated with this family possess planar symmetry with respect to two orthogonal axes; e.g. the pattern shown in figure 4 is symmetric with respect to the horizontal and vertical axes. One can say that this family branches off from the diffuse mode not directly but rather through the chain of sequential bifurcations which occur at points a_1 and d_1.

The long-dashed line in figure 4 represents a family of 3D modes with three symmetrically positioned spots on the periphery, which branches off from the first 2D spot mode at the bifurcation point d_2 or, as one can say, branches off from the diffuse mode through the chain of sequential bifurcations which occur at points a_1 and d_2. The absence of a central spot in patterns associated with this mode is a consequence of the bifurcation point d_2 being positioned on the branch without a central spot of the first 2D spot mode.

Another family branches off from the above-described family of 3D modes with a spot at the centre and two spots on the periphery at the bifurcation point e_1. This family is depicted by the four-dot-dashed line and is associated with patterns that possess planar symmetry with respect to one axis and comprise two spots positioned opposite each other, one of these spots being at the periphery and the other an inside spot. Again, one can say that the family being considered branches off from the diffuse mode not directly but rather through the chain of sequential bifurcations which occur at points a_1, d_1 and e_1.

The above results refer to the limiting case of the reflecting wall of the glow discharge tube or insulating lateral surface of arc cathode, $s = 0$. Results of numerical calculations of multiple modes for the case of the absorbing wall of the glow discharge tube or energy- and current-collecting lateral surface of the arc cathode, $s = 1$, can be found in [33] or [28], respectively. 1D modes do not exist in this case. There are several disconnected 2D modes, one existing at all currents and the others in limited current ranges, and 3D modes existing in limited current ranges.

In all the above-described cases, there is one mode of steady-state current transfer that exists at all discharge currents: the 1D mode in the case $s = 0$ and one of the 2D modes in the case $s = 1$; all the other modes exist in limited current ranges. The 1D mode possesses the highest symmetry of all the modes possible in the case $s = 0$, which are 1D, 2D and 3D. Similarly, 2D modes possess the highest symmetry of all the modes possible in the case $s = 1$, which are 2D and 3D. Therefore, one can say that there is one mode of the highest symmetry admitted by the discharge which exists at all discharge currents, and this is true for both glow discharge and arc cathode. Let us designate this mode the fundamental mode. The importance of the concept of fundamental mode stems from the fact that this is the only mode that exists at currents high and (in the case of glow discharge) low enough and, being the only such mode, it is presumably stable there. Therefore, the discharge at high and (in the case of glow discharge) low currents must operate in the fundamental mode. With a decrease or an increase in current the fundamental mode may turn, or not, unstable and give way to other modes.

2.3. *Identifying bifurcations encountered*

The numerical solutions shown in figures 3 and 4 manifest a large number of bifurcations of different types (a brief description of basic types of steady-state bifurcations is given in appendix A). Many of these bifurcations are fold, i.e. turning points; as an example, turning points of the first 2D spot mode are marked in figure 3(*a*) and turning points of the 3D modes with one and two spots at the periphery are marked in figure 4. All the bifurcations that are not fold involve branching of modes of different symmetries: 2D modes branch off from the 1D modes at the bifurcation points a_1, a_2, ..., a_8, b_1, b_2, ..., b_8 in figure 3 and a_1 in figure 4; 3D modes branch off from the 1D mode at the bifurcation points c_1, c_2 and c_3 in figure 4; 3D modes branch off from the 2D mode at the bifurcation points d_1 and d_2 in figure 4; 3D modes with the period 2π branch off from 3D modes with the period π at the bifurcation point e_1 in figure 4.

A bifurcation $\{2D, 3D\}$ represents breaking of axial symmetry: a continuum of non-symmetric solutions, which are related by the transformation of rotation, branches off from an axially symmetric solution. This must be a pitchfork bifurcation similar to those described by equation (13) in appendix A.1 and shown in figures 14(*c*) and (*d*), with the difference that the number of bifurcating solutions is infinite in this case.

A bifurcation $\{1D, 2D\}$ represents breaking of symmetry of another kind: invariance with respect to translations in the radial direction. This invariance is a property of a particular

mode rather than of the problem, therefore only one 2D mode bifurcates here. In other words, this bifurcation involves two modes and is transcritical. Since there are no reasons for the modes to be tangent at the bifurcation point, this should be a transcritical bifurcation of first-order contact, described by equation (12) and shown in figure 14(*b*).

Breaking of invariance with respect to translations in the radial direction also occurs in a bifurcation $\{1D, 3D\}$. However, this bifurcation represents simultaneously breaking of axial symmetry. Therefore, a continuum of 3D modes which are related by the transformation of rotation bifurcates here and the bifurcation must be pitchfork.

The bifurcation $\{3D, 3D\}$ represents breaking of planar symmetry: two 3D modes possessing planar symmetry with respect to only one (and the same) axis branch off from each 3D mode possessing planar symmetry with respect to two orthogonal axes. This bifurcation again must be pitchfork.

In the vicinity of turning points, the topology of the CVCs shown in figures 3 and 4 is similar to that illustrated by figure 14(*a*) (or by its reflection with respect to the x_0-axis). As far as transcritical bifurcations of first-order contact are concerned, one should expect to encounter intersecting lines as shown in figure 14(*b*). However, no intersections at points a_i and b_i are seen in figures 3 and 4. Furthermore, in cases where the resolution is sufficient, as is the case of bifurcation points b_1 in figure 3(*a*) and a_1 in figure 4, one can clearly see that the CVCs of the diffuse mode and the 2D spot modes are tangent at the bifurcation point rather than intersect. Similarly, the topology of the CVCs in the vicinity of the bifurcation points c_1, c_2, d_1 and e_1 in figure 4 is clearly different from that of pitchfork bifurcations shown in figure 14(*c*) or (*d*).

The above differences are not surprising, since not every functional relation can play the role of a bifurcation diagram in problems with an infinite number of degrees of freedom. Bifurcations involving axially symmetric modes may be conveniently represented in the coordinates (I, j_c), where j_c is the current density at the centre of the cathode. This representation is used in figure 5 in the case of glow discharge. (A convenient feature of this representation is the possibility of easy identification of branches with or without a central spot: they are positioned above or, respectively, below the diffuse mode.) As far as 3D modes are concerned, each continuum would be represented by a single line in these coordinates, just in the same way as in the CVC plane (I, U). Adequate and convenient for 3D modes are coordinates (I, j_e), where j_e is the current density at a fixed point at the edge of the front surface of the cathode, say, at $(r = R, \phi = 0, z = 0)$. This representation is used in figure 6 in the case of the arc cathode. Only two limiting lines are shown for each continuum of 3D modes, one corresponding to the case where the temperature distribution over the edge of the front surface of the cathode, $T(R, \phi, 0)$, has at $\phi = 0$ a maximum and the other a minimum. The families of modes with three spots on the periphery that branch off at the points c_3 and d_2 are not shown in order not to overload the figure.

The solid lines in figures 5 and 6 represent the diffuse mode as before. One can see that the topology of the modes in the vicinity of the bifurcation points b_i in figure 5(*a*) and a_1 in figure 6 indeed is similar to that illustrated by figure 14(*b*) (or by its reflection with respect to the μ-axis) and the topologies of the modes in the vicinity of the bifurcation points c_1 and d_1 in figure 6 are similar to those shown in figure 14(*c*) or (*d*). Appropriate amplifications show that the topologies of the modes in the vicinity of the bifurcation points in figure 5(b) and points c_2 and e_1 in figure 6 are similar to those shown in figures 14(*b*) and, (*c*) or (*d*), respectively. An example of such an amplification is shown in figure 5(*c*). Also shown in the latter figure is the current density at the periphery of the cathode. One can see that the current densities at the centre and at the periphery become equal at the bifurcation point as they should.

Note that the plateau in the dependence $j_c(I)$ corresponding to the first 2D spot mode in figure 5(*a*) is a manifestation of the effect of normal current density, as is the plateau in the CVC of the first 2D spot mode in figure 3(*a*). This effect is manifested also by higher modes; however, it weakens with an increase in the order of the mode and finally disappears.

In the following sections, the bifurcations identified above will be discussed in some detail. Also discussed will be transcritical bifurcations $\{1D, 2D\}$ and $\{2D, 2D\}$ of second-order contact encountered in the modelling of glow discharge [33] and non-cylindrical arc cathodes [19, 20], respectively.

3. Fold bifurcations

A fold, or saddle–node, bifurcation represents not branching of essentially different modes but rather a turning point of the same mode. The importance of understanding these bifurcations originates in their relation with stability of current-controlled discharges. This relation may be explained as follows. Let $f = \tilde{f}(\boldsymbol{r}; U)$ be a family of solutions describing a particular steady-state mode of current transfer. (Here $\boldsymbol{r}$ is the space vector and f designates as before the set of quantities n_i, n_e, φ in the case of glow discharge and T in the case of arc cathode.) Suppose that one substitutes $f = \tilde{f}(\boldsymbol{r}; U)$ into the corresponding boundary-value problem described in section 2.1 with the discharge current I being the control parameter, and differentiates the obtained equations and boundary conditions with respect to U. One will arrive at a problem comprising a linear boundary-value problem for the function $\frac{\partial \tilde{f}(\boldsymbol{r};U)}{\partial U}$ and an expression for parameter $\frac{DI}{DU}$ in terms of the function $\frac{\partial \tilde{f}(\boldsymbol{r};U)}{\partial U}$, where $\frac{DI}{DU}$ is the derivative evaluated along the steady-state mode being considered. At a turning point, this derivative vanishes and the former problem may be viewed as a homogeneous problem for the function $\frac{\partial \tilde{f}(\boldsymbol{r};U)}{\partial U}$ supplemented with a normalization condition for this function. This homogeneous problem coincides with the eigenvalue problem governing stability against small perturbations of a current-controlled discharge with the growth increment equal to zero. Thus, at a turning point the function $\frac{\partial \tilde{f}(\boldsymbol{r};U)}{\partial U}$ represents an eigenfunction of the stability problem associated with the zero eigenvalue (growth increment). In a general case, this

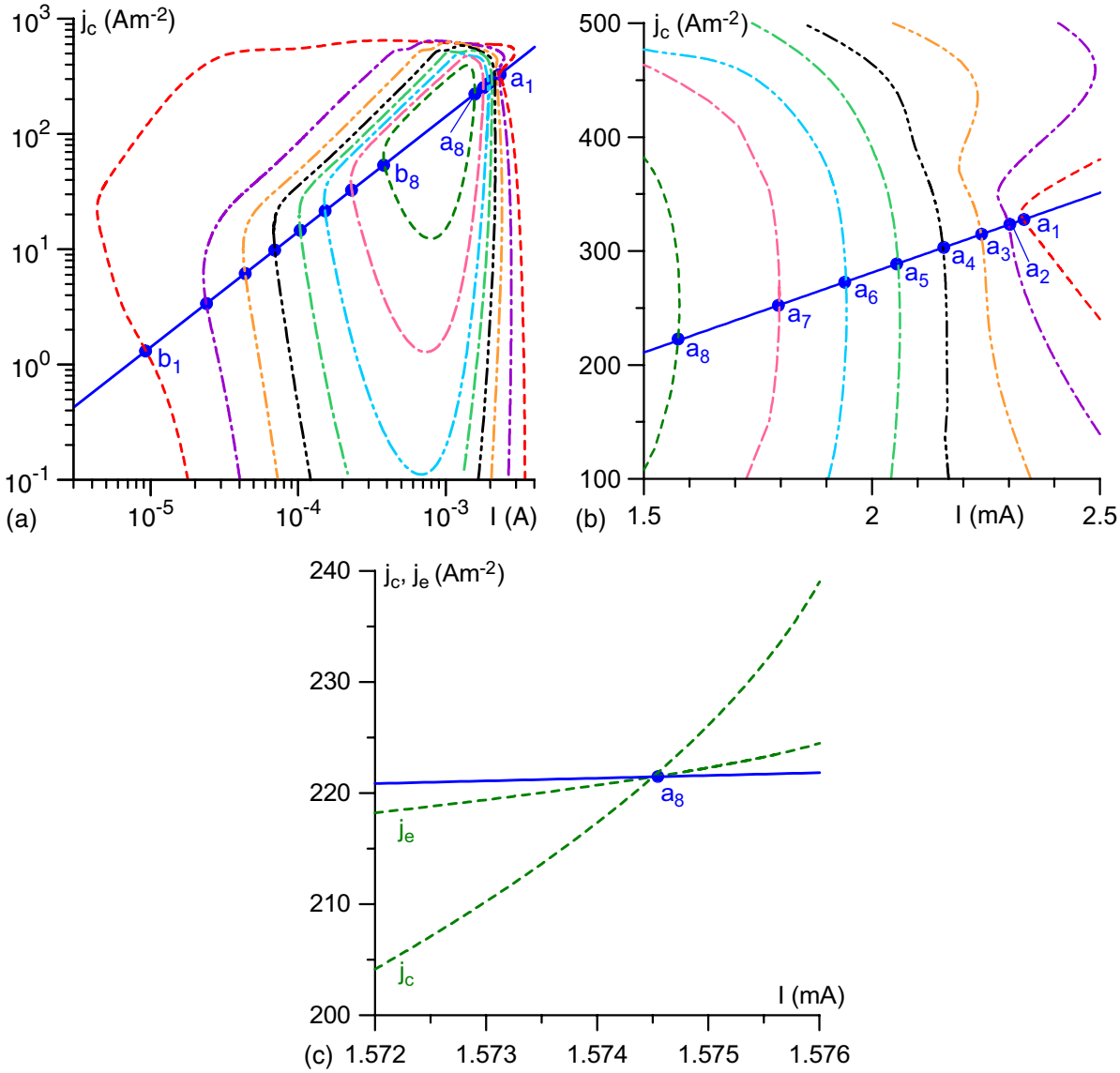

Figure 5. Bifurcation diagram: glow discharge, $s = 0$. (*a*) General view. (*b*) Details in the vicinity of the point of minimum of the CVC of the diffuse mode. (*c*) Details in the vicinity of the bifurcation point a_8 of (*b*).

means that a steady-state mode of current transfer in a current-controlled discharge at a turning point changes stability against a mode of perturbations that at the turning point is described by the function $\frac{\partial \tilde{f}(r;U)}{\partial U}$. In the following, this perturbation mode will be referred to as fundamental.

It is well known that a non-linear electric circuit with inductance is stable if the total differential resistance of the circuit is positive. By analogy, one can assume that a steady state belonging to the falling section of the CVC of any mode of a gas discharge is stable if the external resistance (ballast) is high enough to compensate the negative differential resistance of the discharge in the state in question. Applying this criterion to the limiting case of a current-controlled discharge, where the external resistance is very high, one arrives at the following rule: if a turning point in the plane (I, U) is traversed in the clockwise direction, states before the turning point are stable against the fundamental perturbation mode (in other words, the increment of this perturbation mode is negative) and states after the turning point are unstable (the increment is positive); if the turning point is traversed in the counterclockwise direction, states before the turning point are unstable and states after it are stable. This rule is illustrated by figure 7. Note that scenarios *a* and *b* in figure 7 conform to the second and third scenarios, respectively, of the fold bifurcation mentioned in appendix A.2.

An alternative formulation of the above rule is as follows: the CVC $U(I)$ of a steady-state mode which is stable against perturbations of the fundamental mode can turn only clockwise, after which the steady-state mode becomes unstable; the CVC of an unstable mode can turn only counterclockwise, after which the mode becomes stable.

In the case of the arc cathode, an independent proof of the above rule was given in the analytical stability theory [41]. No such proof has been given up to now in the case of glow discharge; however, the above analogy seems to be sufficiently convincing to consider the rule as a reasonable assumption also in this case.

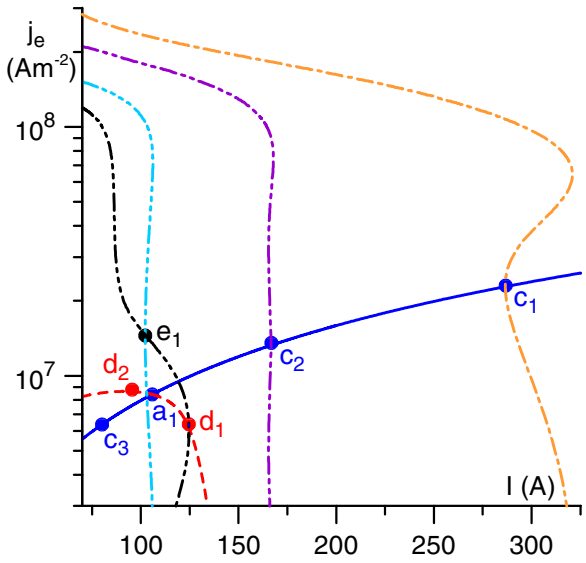

Figure 6. Bifurcation diagram: arc cathode, $s = 0$.

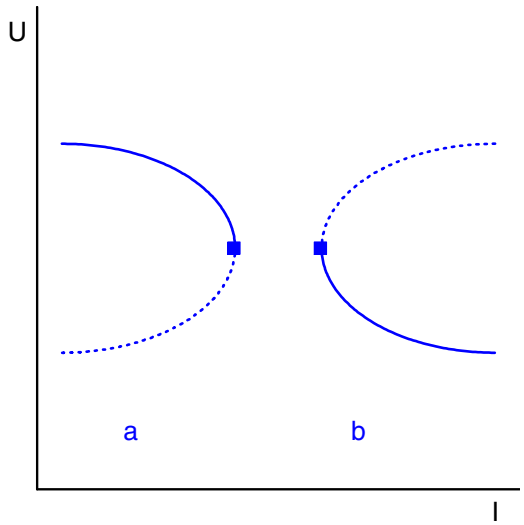

Figure 7. Changes of stability of a steady-state mode of current transfer in the vicinity of a turning point against the fundamental perturbation mode. Solid: stable section of the steady-state mode; dotted: unstable section.

It happens frequently that a steady-state mode manifests more than one turning point. According to the above, there is a change in stability at each point against a mode of perturbations that at the turning point is described by the function $\frac{\partial \tilde{f}(r;U)}{\partial U}$. It seems legitimate to assume that the perturbation mode against which the change in stability occurs is the same for all turning points of the steady-state mode in question or, in other words, that there is only one fundamental perturbation mode for each steady-state mode. (In the case of arc cathode, this assumption was confirmed by the numerical modelling [42].) Then the changes in stability against the fundamental perturbation mode alternate at consecutive turning points: if a steady-state mode has become stable (unstable) on passing through a turning point, it will become unstable (stable) on passing through the next one. Furthermore, directions of turns must alternate: a clockwise turn at one turning point is followed

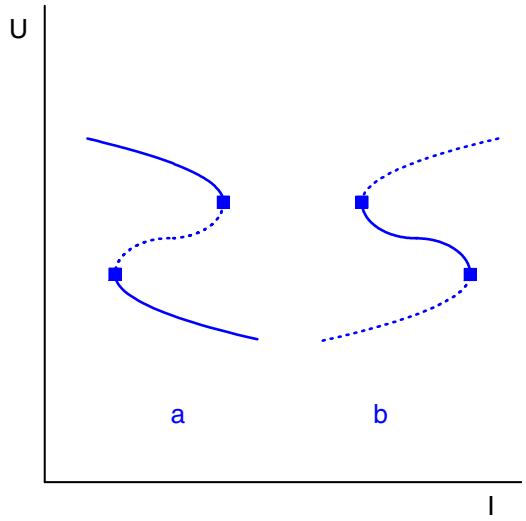

Figure 8. Scenarios of passage of a steady-state mode through two consecutive turning points. Solid: sections of the steady-state mode that are stable against the fundamental perturbation mode; dotted: unstable sections.

by a counterclockwise turn at the next one and vice versa; 360°-loops cannot occur. Possible scenarios of passing through two consecutive turning points are shown in figure 8 and comprise a Z-shape (scenario a) and an S-shape (scenario b).

The above reasoning refers to the case of a current-controlled discharge. A similar reasoning may be developed for the case of a voltage-controlled discharge, with an application to the behaviour of steady-state modes in the vicinity of extrema of the CVC $U(I)$. The conclusion is similar to the above one: a steady-state mode which is stable against perturbations of the fundamental mode can turn only clockwise, and an unstable mode can turn only counterclockwise. However, this line of reasoning seems to give only trivial results.

4. Transcritical bifurcations

4.1. Transcritical bifurcations of first-order contact

Transcritical bifurcations $\{1D, 2D\}$ were studied in [43] for a glow discharge and in [44] for an arc cathode. In both cases, the solutions describing the bifurcating 2D mode are given in the vicinity of bifurcation points a_i and b_i ($i = 1, 2, \ldots$) by the formula

$$\tilde{f}^{(2D)}(r, z; U) = \tilde{f}^{(1D)}(z; U) + C_i(z)\, J_0\left(j'_{0,i+1}\frac{r}{R}\right)(U - U_i) + D_i(r, z)\,(U - U_i)^2 + \cdots, \quad (4)$$

where $\tilde{f}^{(1D)}(z; U)$ and $\tilde{f}^{(2D)}(r, z; U)$ are solutions describing the diffuse and, respectively, 2D spot modes bifurcating at the point considered, $C_i(z)$ and $D_i(r, z)$ are functions of z and, respectively, r and z (or, in the case of glow discharge, a set of functions of z and, respectively, a set of functions of r and z) which depend on the bifurcation point being considered, U_i is the value of the voltage corresponding to the bifurcation point, $J_\nu(x)$ here and further designates Bessel function of the first kind of order ν and $j'_{\nu,m}$ is the mth zero of its derivative.

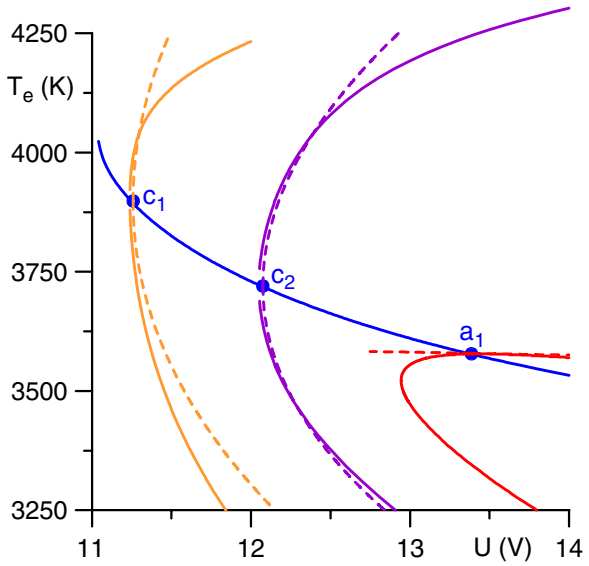

Figure 9. Bifurcations $\{1D, 2D\}$ and $\{1D, 3D\}$: arc cathode, $s = 0$. Solid curves: numerical modelling; dashed curves: analytic approximations.

The conclusion that in the vicinity of a bifurcation point radial variation of the bifurcating 2D mode is proportional to $J_0(j'_{0,i+1}r/R)$ conforms to results of the numerical modelling. For the case of arc cathode, the function $C_i(z)$ was analytically calculated and thus the second term of expression (4). The obtained two-term analytic approximation in the vicinity of the bifurcation point a_1 shown in figures 4 and 6 is depicted by the dashed line in figure 9 and conforms to the numerical modelling as it should.

The behaviour which is typical for transcritical bifurcations of first-order contact and shown in figure 14(*b*) originates in the second term of expression (4). When the expression is averaged over the cathode surface, the contribution of this term vanishes, which follows from the fact that this term was obtained [43, 44] by solving the Neumann problem for the Helmholtz equation and the average value of such solutions is zero. (Of course, this can be derived also from properties of integrals of the Bessel functions.) This explains why CVCs do not represent a proper diagram of transcritical bifurcations in the considered problem, and also why the CVCs of the diffuse and 2D spot modes are tangent at the bifurcation point as seen in figures 3 and 4.

Results of a numerical investigation of stability of the diffuse (1D) and 2D spot modes of current transfer to an arc cathode and of an analytical investigation of stability of the diffuse mode, reported in [42], have revealed an exchange of stability in the vicinity of points of transcritical bifurcation of first-order contact, which is similar to the one occurring in systems with one degree of freedom and illustrated in figure 14(*b*). This exchange is realized as follows: at a bifurcation point, i.e. at $I = I(a_i)$, both the diffuse mode and the 2D spot mode that branches off at a_i are neutrally stable against a 2D perturbation mode with a radial dependence described by the function $J_0(j'_{0,i+1}r/R)$; the diffuse mode is stable and the 2D spot mode is unstable at $I > I(a_i)$; and vice versa at $I < I(a_i)$.

As shown by the numerical modelling [42], the above-mentioned 2D perturbation mode that is neutrally stable at a_i is the same one that changes sign of its increment at all turning points of the steady-state 2D spot mode that branches off at a_i. In other words, it represents the fundamental perturbation mode of the steady-state 2D spot mode in question. Note that this perturbation mode, while being proportional to $J_0(j'_{0,i+1}r/R)$ in all states of the diffuse mode, is no longer proportional to $J_0(j'_{0,i+1}r/R)$ in states of the 2D steady-state spot mode outside the bifurcation point a_i.

It is natural to assume that in the case of glow discharge the above conclusions on stability apply to the bifurcation points a_i. The exchange of stability at bifurcation points b_i presumably occurs in the opposite direction: at $I < I(b_i)$, the diffuse mode is stable against the perturbation mode which is fundamental for the steady-state 2D spot mode in question and the 2D spot mode is unstable; and vice versa at $I > I(b_i)$.

4.2. Perturbed transcritical bifurcations of first-order contact

Analysis of the preceding section refers to the limiting case $s = 0$ (reflecting wall of a glow discharge tube and insulating lateral surface of an arc cathode). Deviations of s from zero represent imperfections that should break the bifurcations as described in appendix A.3. This is indeed found in the numerical modelling as shown in figures 10 and 11. Values of s chosen for figures 10(*a*), (*b*) and 11 are all different in order that the diagrams be transparent. Also shown in these figures are the diffuse mode and the first 2D spot mode for $s = 0$, and in figure 10(*b*) also the second 2D spot mode for $s = 0$ is shown.

The effect of imperfection at each bifurcation point is the same as discussed in appendix A.3 and shown in figure 15(*a*): two bifurcating solutions are broken into two isolated solutions with the branches exchanged. In the case of glow discharge, the first scenario discussed in appendix A.3 and illustrated by figure 15(*a*) with $\delta \geqslant 0$ takes place at bifurcation points $a_2, a_4, a_6, a_7, b_1, b_3, b_5, b_7$ and the second scenario (figure 15(*a*) with $\delta \leqslant 0$) occurs at $a_1, a_3, a_5, a_8, b_2, b_4, b_6, b_8$. The sections of the diffuse mode $I < I(b_1)$ and $I > I(a_1)$ join the central-spot branch of the first 2D spot mode. The sections of the diffuse mode $I(b_1) < I < I(b_2)$ and $I(a_2) < I < I(a_1)$ join, on one hand, the branch with a ring spot on the periphery of the first 2D spot mode, and on the other hand, the branch with an inside ring spot of the second 2D spot mode. The sections of the diffuse mode $I(b_2) < I < I(b_3)$ and $I(a_3) < I < I(a_2)$ join, on one hand, the branch with a central spot and a ring spot on the periphery of the second 2D spot mode, and on the other hand, the branch with a central spot and an inside ring spot of the third 2D spot mode. This pattern is repeated and finally the section $I(b_8) < I < I(a_8)$ joins the branch with a central spot, three inside ring spots and a ring spot on the periphery of the eighth 2D spot mode.

In the case of arc cathode, the second scenario occurs at a_1. The section of the diffuse mode $I > I(a_1)$ joins the branch with a ring spot on the periphery of the first 2D spot mode and the section of the diffuse mode $I < I(a_1)$ joins the branch with a central spot. Also shown in

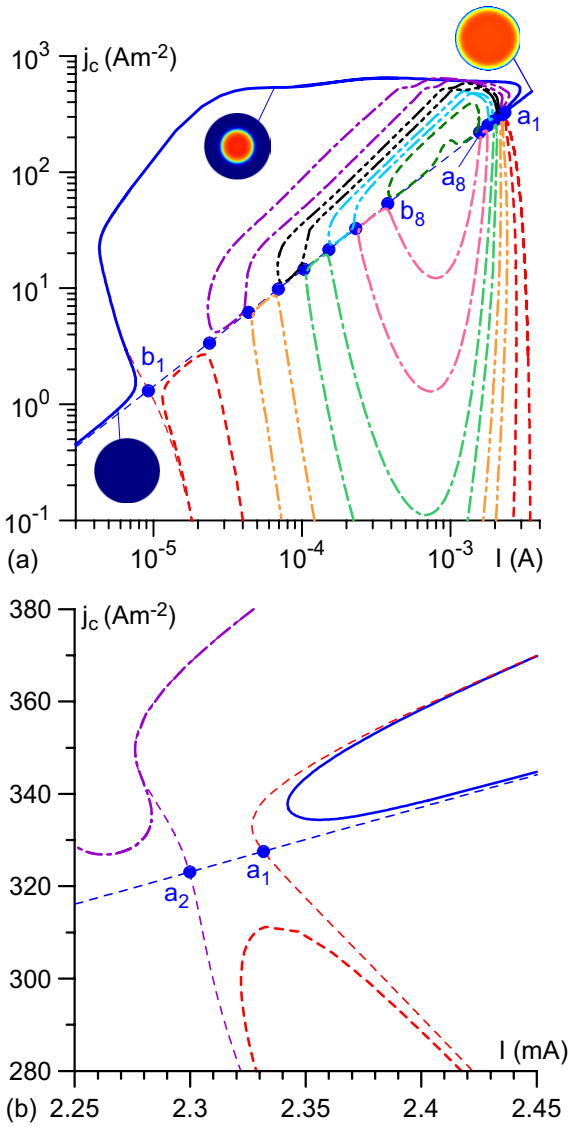

Figure 10. Bifurcation diagram and schematics of current density distribution over the cathode surface in the fundamental mode. Perturbed transcritical bifurcation of first-order contact, glow discharge. (*a*) General view, $s = 0.05$. (*b*) Details in the vicinity of the point of minimum of the CVC of the diffuse mode, $s = 0.01$.

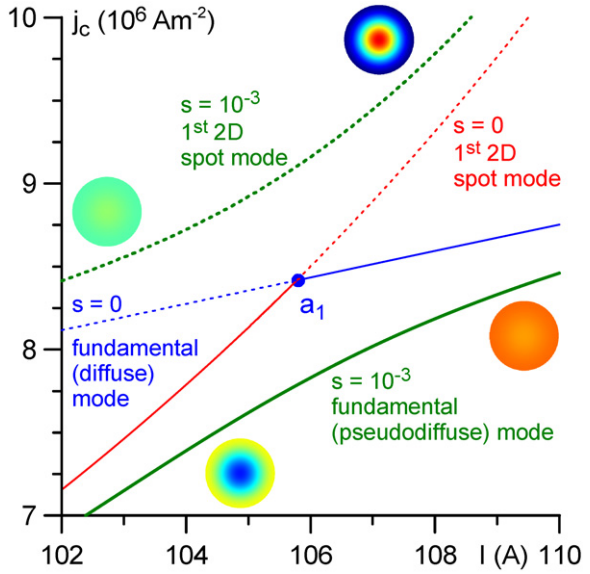

Figure 11. Bifurcation diagram and schematics of current density distribution over the front surface of the cathode. Perturbed transcritical bifurcation of first-order contact, arc cathode, $s = 10^{-3}$. Solid: sections of the steady-state modes that are stable against axially symmetric perturbations; dotted: unstable sections.

figure 11 is a pattern of stability against axially symmetric perturbations (more precisely, against the first mode of axially symmetric perturbations) obtained in the numerical modelling; it conforms to figure 15(*a*) with $\delta \leqslant 0$ as it should.

One of the consequences of the above-described exchange of branches is that the fundamental mode, i.e. the mode that exists at all I, is no longer diffuse and may be not even close to diffuse: it comprises section(s) of the diffuse mode (or, more precisely, what was the diffuse mode at $s = 0$) and one of the branches of the first 2D spot mode, namely, the branch with a central spot in the case of glow discharge and the branch with a ring spot on the periphery in the case of arc cathode. The fact that the branches are not the same originates in different physics introduced by boundary conditions at $r = R$ in the cases of glow discharge and arc cathode. A non-reflecting wall of a glow discharge tube reduces local intensity of the glow discharge due to losses of the charged particles caused by diffusion to the wall. As a consequence, the diffuse discharge becomes less intense on the periphery than at the centre. Thus, the diffuse mode acquires some similarity with the branch with a spot at the centre, and it is not surprising that the two join. On the contrary, energy- and current-collecting lateral surface of an arc cathode provides an additional (lateral) heating of the edge of the front surface and thus locally enhances the discharge. As a consequence, the diffuse discharge becomes more intense at the edge than at the centre. Thus, the diffuse mode acquires some similarity with the branch with a ring spot on the periphery, and it is not surprising that the two join.

The above-described difference between the fundamental modes for $s \neq 0$ in the cases of glow discharge and arc cathode is seen in the schematics of distributions of the current density shown in figures 10(*a*) and 11. At high currents, $I \gtrsim I(a_1)$, the distributions are more or less uniform in both the cases; however, there is a minimum of the current density on the periphery in the case of glow discharge and a maximum in the case of arc cathode. The difference is increased at lower currents, $I \lesssim I(a_1)$: a well-pronounced spot appears at the centre of the glow cathode while the maximum of the current density on the periphery of the arc cathode becomes better pronounced.

A further difference between the fundamental modes at $s \neq 0$ and $I \lesssim I(a_1)$ in the cases of glow discharge and arc cathode is as follows. The fundamental mode in the case of glow discharge manifests a well-pronounced effect of normal current density, which is attested, in particular, by a plateau in the dependence $j_c(I)$ (solid line in figure 10(*a*)) at $30\,\mu\text{A} \lesssim I \lesssim 3\,\text{mA}$. Nothing of this kind is manifested by the fundamental mode on the arc cathode. This difference stems from the strongly different aspect ratios. The effect of normal current density is a particular case of coexistence of phases which is possible in wide systems. In the case of

glow discharge, the characteristic dimension in the z-direction is represented by the interelectrode gap or the thickness of the near-cathode space-charge sheath, whichever is smaller. The thickness of the near-cathode space-charge sheath under conditions of the above-mentioned plateau in the dependence $j_c(I)$ corresponding to the fundamental mode is approximately 0.13 mm, which is much smaller than the discharge radius R. Thus, the system represented by the glow discharge indeed may be considered as wide. In the case of arc cathode, the characteristic dimension in the z-direction is the cathode height h, so the aspect ratio h/R is 5. Thus, the arc cathode represents a narrow rather than wide system and it is not surprising that it does not manifest the effect of normal current density.

All the steady-state modes in the case $s \neq 0$ other than the above-described fundamental mode exist in limited current ranges and in the case of glow discharge continue to represent closed loops. The topology of these modes may be understood by means of the same reasoning as above. In particular, the intensity of a ring spot on the periphery is locally reduced in the immediate vicinity of the wall of a glow discharge tube, thus the structure acquires some similarity with an inside ring spot and this is why the corresponding branches join the same section of the diffuse mode.

As s increases from the value of 0.05 shown in figure 10(a) up to unity in the case of glow discharge, the above-described fundamental mode does not suffer dramatic changes. This is illustrated by figure 1. A dotted line in this figure depicts the CVC of the fundamental mode for $s = 0.05$; however, it is virtually indistinguishable from the solid line, which corresponds to $s = 1$, except in the vicinity of transitions from the Townsend discharge to the subnormal mode and from the normal to the abnormal modes. The range of currents in which each non-fundamental 2D mode shown in figure 10 exists shrinks with increasing s and higher order modes disappear one by one. Only two initial modes remain in existence at $s = 1$, the mode with an inside ring spot and the one with a central spot and an inside ring spot [33].

The CVC of the fundamental mode on an arc cathode with $s = 1$ is quite close to the CVC of the diffuse mode on a cathode with $s = 0$, shown in figure 4, if the discharge current does not exceed, say, 500 A. Differences between the temperature of the cathode surface in these two modes reach about 400 K. The CVC of the first non-fundamental 2D mode on arc cathode with $s = 1$ also is close to the CVC of the first 2D spot mode mode on a cathode with $s = 0$, shown in figure 4, although differences in the surface temperature reach about 1000 K.

Distributions of the surface temperature of an arc cathode with an energy- and current-collecting lateral surface, $s = 1$, in four states corresponding to the same near-cathode voltage drop $U = 15$ V are shown in figure 12. (Note that the range $0 \leqslant r+z \leqslant 2$ mm in this figure corresponds to the front surface of the cathode, the range $r+z \geqslant 2$ mm corresponds to the lateral surface.) The states with the discharge currents of 77.14 A and 23.55 kA belong to the fundamental mode. In the latter state, the temperature is very high and constant ('saturated') along the front surface and the most part of the lateral surface; a feature which is characteristic for the high-current section of the fundamental mode [25]. There is something resembling a

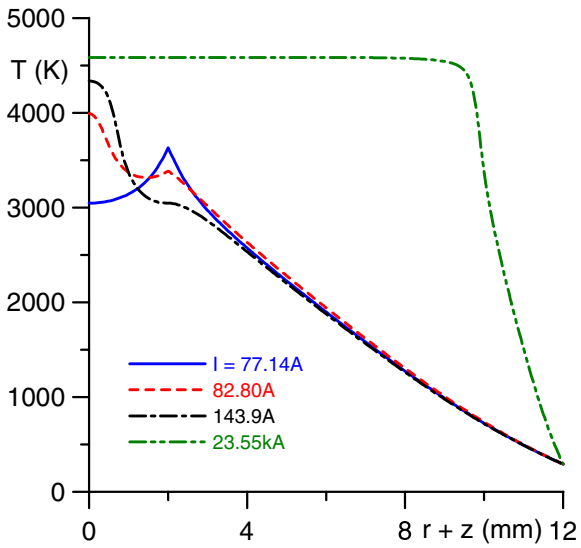

Figure 12. Distributions of temperature of the surface of an arc cathode. $s = 1$, $U = 15$ V.

ring spot attached to the edge of the front surface of the cathode in the state with $I = 77.14$ A. The states with $I = 82.80$ and 143.9 A belong to the first non-fundamental 2D mode. There is a central spot in the latter state and a central spot and something resembling a ring spot at the edge in the former state. One can say that all four states bear footprints of their origin. In particular, the pattern revealed by the state with $I = 82.80$ A is similar to the pattern associated with one of the branches of the second 2D spot mode, namely, the branch with a central spot and a ring spot at the edge, which, jointly with the diffuse mode and the branch with a central spot of the first 2D spot mode, originates the first non-fundamental 2D spot mode. This similarity is remarkable, given that the bifurcation point a_2 at which the second 2D spot mode branches off from the diffuse mode is not present within the range of U considered in this work.

Variations of temperature along the front surface of the cathode operating in the fundamental mode under conditions of figure 12 are moderate, and they are still smaller for thinner cathodes, which are used in arc lamps and are best studied experimentally. The thermal regime of the cathode does not appear to be spot-like but rather looks diffuse. As a consequence, the above-described difference between the fundamental modes on cylindrical arc cathodes with insulating and active lateral surfaces has not been appreciated up to now and both are termed 'diffuse' in the preceding works. In this work, the fundamental mode on a cylindrical arc cathode with $s \neq 0$ is termed 'pseudodiffuse' in order to distinguish it from the fundamental mode in the case $s = 0$ (which is associated with a uniform distribution of discharge parameters along the cathode surface, i.e. is truly diffuse). The first non-fundamental 2D mode at $s \neq 0$ is termed the first 2D spot mode.

4.3. Transcritical bifurcations of second-order contact

Numerical modelling of glow discharge [33] revealed that a decrease in the radius of the discharge tube with reflecting

wall causes 2D spot modes to disappear one by one, starting from the higher order modes. The disappearance of each mode occurs through shrinking of the current range in which the mode exists. At first, shrinking occurs while the spot mode remains connected to the diffuse mode, then the spot mode detaches from the diffuse mode and shrinking continues until the spot mode disappears completely. An example illustrating this detachment is shown in figure 13(*a*). (Here $\langle j \rangle$ designates the average current density to the cathode surface. Since dependence $j_c(\langle j \rangle)$ for the diffuse mode is the same for tubes of different radii, there is only one solid line in this figure.) The 2D spot mode and the diffuse mode are connected at two first-order transcritical bifurcation points at $R \gtrsim 0.527$ mm. The two bifurcation points merge to form a transcritical bifurcation of second-order contact when R has decreased down to a certain value around 0.527 mm. The 2D spot mode and the diffuse mode become disconnected at $R \lesssim 0.527$ mm.

The topology of modes in figure 13(*a*) is similar to that shown in figure 15(*c*). One can conclude that the above-described detachment of a 2D spot mode from the diffuse mode occurs through a perturbed transcritical bifurcation $\{1D, 2D\}$ of second-order contact according to the scenario shown in figure 15(*c*).

Numerical modelling of arc cathodes of shapes of industrial interest [19, 20] revealed a possibility of dramatic changes in the pattern of steady-state modes of current transfer. As an example, figure 13(*b*) shows the temperature at the centre of the front surface of a cathode having the shape of a rod (cylinder) with a hemispherical tip. The cathode radius is variable, the cathode height is 10 mm, the whole front and lateral surface is energy- and current-collecting, all the other parameters are the same as indicated in section 2.1. One can see that the pseudodiffuse and the first 2D spot modes, representing separate modes at $R \lesssim 1.169$ mm, become connected when R has increased up to a certain value around 1.169 mm, then they exchange branches and separate once again. Each of these two new disconnected modes embraces states typical for both diffuse and spot modes [19, 20] and cannot be termed (pseudo)diffuse or spot mode. On the other hand, one of these modes exists at all values of the discharge current and may be termed fundamental mode.

The topology of modes in figure 13(*b*) is similar to that shown in figure 15(*b*): a transcritical bifurcation of second-order contact occurs at $R \approx 1.169$ mm, small deviations of R from this value break the bifurcation. The pattern of stability also is similar. One can conclude that the above-described change in pattern of steady-state modes of current transfer occurs through a perturbed transcritical bifurcation $\{2D, 2D\}$ of second-order contact according to the scenario shown in figure 15(*b*).

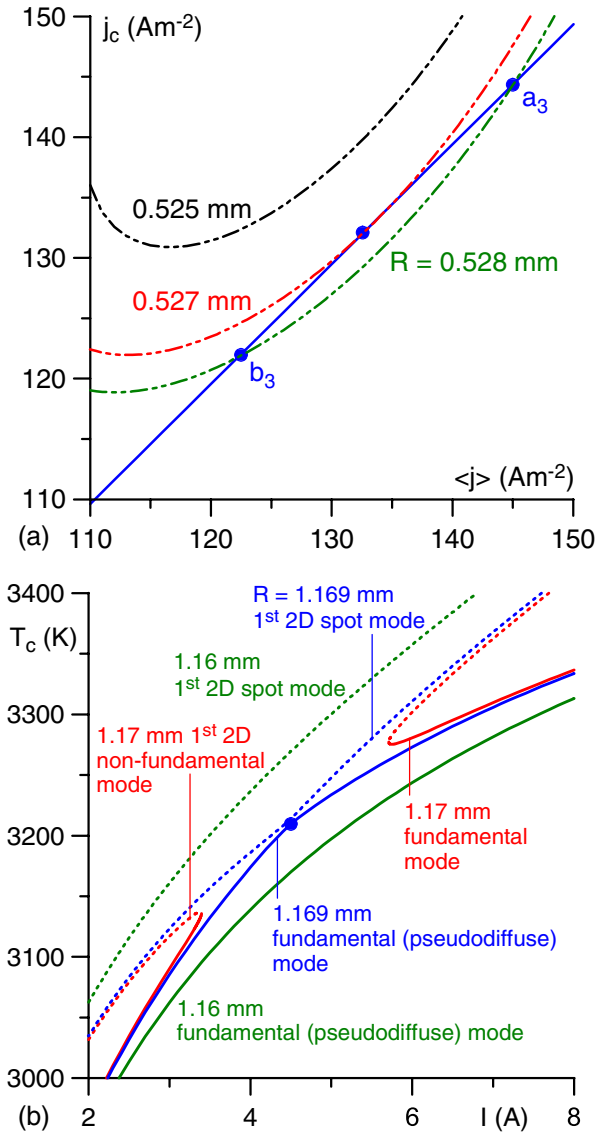

Figure 13. Bifurcation diagrams, perturbed transcritical bifurcation of second-order contact. (*a*) Glow discharge, $s = 0$. Solid: diffuse mode; two-dot-dashed: third 2D spot mode. (b) Arc cathode with a hemispherical tip. Solid: (absolutely) stable sections of the steady-state modes; dotted: unstable sections.

5. Pitchfork bifurcations

Pitchfork bifurcations $\{1D, 3D\}$ were treated in [43] for a glow discharge and in [44] for an arc cathode. In both cases, the solutions describing the bifurcating 3D modes are given in the vicinity of bifurcation points c_i $(i = 1, 2, \ldots)$ by the asymptotic expansion

$$\tilde{f}^{(3D)}(r, \phi, z; U) = \tilde{f}^{(1D)}(z; U_i) + C_i(z)\, J_\nu\left(j'_{\nu,m}\frac{r}{R}\right) \times \cos(\nu\phi + \alpha)\sqrt{|U - U_i|} + D_i(r, \phi, z)(U - U_i) + \cdots, \tag{5}$$

where $\tilde{f}^{(3D)}(r, \phi, z; U)$ is a solution describing the 3D spot modes bifurcating at the point considered, ν is an integer equal to i at $i \leqslant 4$ and below i at $i > 4$, $m = 1, 2, \ldots$, α is an arbitrary constant, $C_i(z)$, $D_i(r, \phi, z)$ and U_i have the same meaning as above except that $D_i(r, \phi, z)$ depends also on ϕ. The conclusion that in the vicinity of a bifurcation point transversal variations of the bifurcating 3D modes are proportional to $J_\nu(j'_{\nu,m} r/R)\cos(\nu\phi + \alpha)$ conforms to results of the numerical modelling of 3D modes (which has been performed only for

the case of arc cathode up to now). The order of initial non-trivial zeros of the derivatives of the Bessel functions of the first kind, $j'_{1,1} \approx 1.841$, $j'_{2,1} \approx 3.054$, $j'_{0,2} \approx 3.832$, $j'_{3,1} \approx 4.201$, $j'_{4,1} \approx 5.318$, $j'_{1,2} \approx 5.331, \ldots$, governs the order of branching of different spot modes from the diffuse mode. This is indeed the order detected in the numerical modelling in the case of arc cathode with the insulating lateral surface in the range of currents down to 0.3 A as described in section 2.2.

For the case of arc cathode, the function $C_i(z)$ was analytically calculated and thus the second term of asymptotic expansion (5). The obtained two-term analytic approximation in the vicinity of the bifurcation points c_1 and c_2 shown in figures 4 and 6 is depicted by the dashed lines in figure 9 and conforms to the numerical modelling as it should. Note that there are small gaps in the vicinity of points c_1 and c_2 in the solid lines representing the numerically calculated characteristics of the 3D modes. These gaps stem from divergence of iterations which sometimes occurs in a close vicinity of a bifurcation point.

Pitchfork bifurcations $\{2D, 3D\}$, occurring at the bifurcation points d_1 and d_2 in figures 4 and 6, represent the most frequent type of bifurcations that can occur in cases where 2D modes exist but 1D modes do not (such as the case $s = 1$ or all the cases with non-cylindrical axially symmetric geometries). These bifurcations were treated in [41, 45] for the case of arc cathode. In both the cases of glow discharge and arc cathode, the solutions describing the bifurcating 3D modes are given in the vicinity of bifurcation points d_i $(i = 1, 2, \ldots)$ by the asymptotic expansion

$$\tilde{f}^{(3D)}(r, \phi, z; U) = \tilde{f}^{(2D)}(r, z; U_i) + E_i(r, z)\cos(\nu\phi + \alpha) \times\sqrt{|U - U_i|} + D_i(r, \phi, z)(U - U_i) + \ldots, \quad (6)$$

where $E_i(r, z)$ is a function of r and z (or, in the case of glow discharge, a set of functions) which depends on the bifurcation point being considered. The harmonic azimuthal variation of the bifurcating 3D modes in the vicinity of a bifurcation point, predicted by the theory, was found in the numerical modelling.

The behaviour which is typical for pitchfork bifurcations and shown in figures 14(*c*) and (*d*) originates in the second term of expansion (5) or (6). When the expansion is averaged over the cathode surface, the contribution of this term, which is harmonic in ϕ, vanishes. This explains why the CVCs do not represent a proper diagram of pitchfork bifurcations in the considered problem, and also why the CVCs of the bifurcating 3D spot modes have finite inclinations at the bifurcation points c_1, c_2, d_1 and d_2 in figure 4.

The analytical and numerical investigation of stability of 2D and 3D spot modes of current transfer to an arc cathode, reported in [41, 42], have revealed an exchange of stability in the vicinity of points of pitchfork bifurcation $\{2D, 3D\}$, which is similar to the one occurring in systems with one degree of freedom and illustrated by figures 14(*c*) and (*d*). This exchange is realized as follows. At a bifurcation point, i.e. at $I = I(d_i)$, the 2D steady-state mode and the 3D steady-state modes that branch off at this point are neutrally stable against a 3D perturbation mode with an azimuthal dependence described by the same factor $\cos(\nu\phi + \alpha)$ that describes azimuthal variation of the steady-state 3D modes in the vicinity of the bifurcation point. The 2D mode changes its stability at the bifurcation point, i.e. either it is stable against the above-described 3D perturbation mode at $I > I(d_i)$ and unstable at $I < I(d_i)$, or vice versa. (As far as bifurcation points positioned on the pseudodiffuse mode are concerned, the pseudodiffuse mode is stable at $I > I(d_i)$ and unstable at $I < I(d_i)$.) The 3D modes are stable if they are supercritical, i.e. branch off into the current range where the 2D mode is unstable, and unstable if they are subcritical, i.e. branch off into the current range where the 2D mode is stable. The increments of the above-indicated perturbation of the steady-state 2D mode and 3D modes are related by the formula $\lambda^{(3D)} = -2\lambda^{(2D)}$ in the vicinity of the bifurcation point. This formula coincides with the corresponding relation in systems with one degree of freedom, which follows from equation (20).

As shown by the numerical modelling [42], the above-mentioned 3D perturbation mode that is neutrally stable at d_i is the same one that changes sign of its increment at all turning points of the corresponding steady-state 3D mode that branches off at d_i. In other words, it represents the fundamental perturbation mode of the corresponding steady-state 3D mode. Note that this perturbation mode, while being proportional to $\cos(\nu\phi + \alpha)$ in all states of the 2D mode, is no longer proportional to $\cos(\nu\phi + \alpha)$ in states of the 3D steady-state spot mode outside the bifurcation point d_i.

The pitchfork bifurcation $\{3D, 3D\}$, which occurs on an arc cathode at the point e_1 shown in figures 4 and 6, represents breaking of planar symmetry. For example, symmetry with respect to the horizontal axis is broken in the pattern shown in figure 4, although symmetry with respect to the vertical axis is conserved. The pattern of stability against the fundamental perturbation mode in the vicinity of the bifurcation point conforms to scenario 14(*d*). Note that the possibility of this bifurcation was detected first in the numerical investigation of stability in the case $s = 1$ [42].

A question arises as to how a planar symmetry-breaking bifurcation can transform a three-spot pattern into a two-spot one. This may be explained as follows. At states between the bifurcation points d_1 and e_1, the temperature distribution is symmetric, say, with respect to the vertical and horizontal axes and possesses three maxima, associated with the central spot and two spots on the periphery (although the spots on the periphery are still pronounced extremely weakly: the temperature at its centres exceeds the temperature outside the spots by about 1 K). At the bifurcation point e_1, the central spot starts moving up- or downwards. This movement is accompanied by the complete extinction of the upper (or, respectively, lower) peripheral spot and by the enhancement of the opposite peripheral spot. If the central spot moves upwards, the two-spot pattern shown in figure 4 appears.

It is natural to assume that the above conclusions on bifurcations $\{1D, 3D\}$ and $\{2D, 3D\}$, drawn for the case of arc cathode, apply also to the case of glow discharge. A bifurcation $\{3D, 3D\}$ similar to the one discussed above for the case of arc cathode can occur also in the case of glow discharge.

6. Discussion

The above analysis provides explanations to many results obtained in numerical modelling. One example is the fundamental mode of glow discharge in a tube with absorbing lateral surface depicted by the solid line in figure 1. This is the only mode that exists at currents low or high enough; therefore it should be stable at such currents. Note that this conclusion conforms to the fact that the Townsend and abnormal glow discharges may be observed in the experiment. The (absolute) stability includes stability against the fundamental perturbation mode. Then it follows from analysis of section 3 that transitions from the Townsend discharge to the subnormal mode and from the normal to the abnormal modes must occur either without turning points or with a Z-shape, but not with an S-shape. This is indeed what was found in the modelling as seen in figure 1: the solid line manifests a Z-shape at I around 5 μA and has no turning points at I around 3 mA. The same reasoning applies to the dotted line, and indeed it manifests Z-shapes at I around both 5 μA and 3 mA.

The branch of the first 2D spot mode of glow discharge (figures 3 and 5) which is associated with a ring spot on the periphery possesses one turning point. This point corresponds to $I = 3.4$ mA and is marked by square in figure 3(a). Taking into account the behaviour of the CVC at this turning point and applying the analysis of section 3, one concludes that the section of this branch comprised between the bifurcation point b_1 and the turning point is stable against the fundamental perturbation mode, and the section between the turning point and the bifurcation point a_1 is unstable. This conclusion conforms to the pattern of stability at points of transcritical bifurcation of first-order contact, discussed in section 4.1.

The central-spot branch of the first 2D spot mode of glow discharge possesses three turning points. The first and second ones are marked in figure 3(a) and correspond to $I = 4.3\,\mu$A and $I = 2.9$ mA, respectively. The third turning point is revealed by a further magnification of the vicinity of point a_1 in figures 3(b) and 5(b) and is positioned very close to the bifurcation point a_1. The CVC of the section of the considered branch that is comprised between the bifurcation point b_1 and the third turning point is S-shaped. It follows from analysis of section 3 that the section between b_1 and the first turning point and the section between the second and third turning points are unstable against perturbations of the fundamental mode, the sections between the first and second turning points and between the third turning point and the bifurcation point a_1 are stable. Again, these conclusions conform to the pattern of stability at points of transcritical bifurcation of first-order contact.

A similar reasoning applies to the fundamental mode in the case of arc cathode. This is the only mode that exists at currents high enough, therefore it should be stable at such currents. (This conclusion is confirmed by both the numerical modelling and the experiment.) The steady-state mode with one spot at the periphery of the arc cathode possesses one turning point (square on the dot-dashed line in figure 4). Taking into account the behaviour of the CVC at this point and applying the analysis of section 3, one concludes that the section of this mode comprised between the bifurcation point c_1 and the turning point is unstable against perturbations of one mode (which is the fundamental perturbation mode of the steady-state mode being considered), and the section beyond the turning point is (absolutely) stable. This conclusion conforms to the pattern of stability at points of subcritical pitchfork bifurcation, discussed in section 5, and indeed was found in the numerical modelling.

The CVC of the steady-state mode with two spots at the periphery of the arc cathode (two-dot-dashed line in figure 4) manifests a Z-shape. One concludes that this mode is stable against the fundamental perturbation mode except the section between the turning points. This conforms to the pattern of stability at points of supercritical pitchfork bifurcation, discussed in section 5, and indeed was found in the modelling.

A number of Z-shapes has been found in the modelling [20]. 360°-loops have been found neither in the case of glow discharge nor in the case of arc cathodes.

The following question was discussed in the works [25, 46] in connection with numerical modelling of multiple modes of current transfer to arc cathodes: once multiple modes of current transfer have been found in a certain current range, is there any reason to call one (or several) of them the diffuse mode(s) and others spot modes? It has become clear by now that the answer to this question is negative in a general case. The only mode that can be unambiguously distinguished is the one that exists at all discharge currents and possesses the highest symmetry admitted by the discharge. In the present work, this mode is called fundamental. Note that one could consider also 'composed' modes that exist at all I, for example a mode comprising the sections $I < I(b_1)$ and $I > I(a_1)$ of the 1D mode and one of the branches of the first 2D mode under conditions of figure 3(a); or a mode comprising the section $I > I(c_1)$ of the 1D mode and the 3D mode with one spot at the edge mode under conditions of figure 4. The words 'the highest symmetry admitted by the discharge' mean that such composed modes should not be considered as fundamental.

In the case of a cylindrical glow discharge tube with the reflecting wall or of a cylindrical arc cathode with the insulating lateral surface, $s = 0$, the fundamental mode is associated with a uniform distribution of discharge parameters along the cathode surface, i.e. is diffuse. In the case of a cylindrical arc cathode with an active lateral surface, $s = 1$, the fundamental mode is associated with moderate variations of the temperature along the front surface of the cathode provided that the cathode is thin, so this mode appears more or less diffuse (the pseudodiffuse mode, in terms of this work). The fundamental mode of glow discharge in a cylindrical tube with the absorbing wall, $s = 1$, embraces states with smooth variations of parameters along the cathode surface (the Townsend discharge and the abnormal discharge), but also states with a current spot (the subnormal and normal discharges). Similarly, the fundamental mode on a non-cylindrical arc cathode may embrace states typical for both diffuse and spot modes. One can conclude that the fundamental mode is diffuse or pseudodiffuse in some situations, but is definitely non-diffuse in others. In other words, the concept of fundamental mode does not coincide with the concept of diffuse mode, but rather represents the only meaningful generalization of the latter concept.

A transition between the 1D fundamental mode in the case of a cylindrical glow discharge tube with the reflecting wall or of a cylindrical arc cathode with the insulating lateral surface, $s = 0$, and the 2D fundamental mode in the case of glow discharge in a cylindrical tube with the absorbing wall or of a cylindrical arc cathode with an energy- and current-collecting lateral surface, $s = 1$, is discontinuous. If one starts from a state belonging to the fundamental mode in the case $s = 1$ and then gradually decreases s, one will arrive at $s = 0$ at a state belonging to a 'composed' mode comprising section(s) of the 1D mode and one of the branches of the first 2D spot mode, namely, the branch with a spot at the centre in the case of glow discharge and the branch with a ring spot on the periphery in the case of arc cathode. Similarly, if one starts from the (1D) fundamental mode in the case $s = 0$ and then gradually increases s, one will not necessarily arrive at $s = 1$ at the fundamental mode: one may also arrive at one of the branches of one of the non-fundamental 2D modes, or can obtain no solution at all.

It was shown in section 4.2 that the reason of the above-described discontinuity is an exchange of branches that occurs when the bifurcation $\{1D, 2D\}$ is perturbed and the two bifurcating solutions are broken into two isolated solutions with the branches exchanged.

The above results allow one to answer questions raised in section 1 in connection with figures 1 and 2. The subnormal and normal modes of glow discharge are already present in the case $s = 0$, but they represent a part of the first 2D spot mode rather than of the fundamental mode. They become a part of the fundamental mode after the exchange of branches. On the contrary, the mode which is described by the von Engel and Steenbeck solution and is associated with the falling section of the CVC represents a part of the fundamental mode at $s = 0$, but becomes divided between different non-fundamental 2D modes after the exchange of branches. The procedure of simulations with the use of the built-in initial approximation implemented in the Internet tool [2] amounts to a transition from the fundamental (diffuse) mode at $s = 0$ to $s = 1$. This transition leads to the fundamental (pseudodiffuse) mode at $s = 1$ provided that U is below the value corresponding to the point at which the bifurcation $\{1D, 2D\}$ occurs (point a_1 in figures 4 and 6), and 13.46 V is precisely this value. In the range of U above the point of minimum of the CVC of the first 2D spot mode in the case $s = 1$, which is 14.04 V, the transition leads to the low-voltage branch of the first 2D spot mode at $s = 1$. The fundamental mode in the case $s = 0$ has no analogue in the case $s = 1$ in the range of voltages $13.46\,\mathrm{V} \lesssim U \lesssim 14.04\,\mathrm{V}$, whence the lack on convergence in this range of voltages.

The fundamental mode in a glow discharge with $s = 1$ manifests a normal spot and could hardly be confused with the fundamental mode in the case $s = 0$, which is diffuse. Due to a substantially different aspect ratio, the situation in the case of arc cathode is different: the fundamental mode on an arc cathode with $s = 1$ is characterized by modest variations of parameters along the front surface of the cathode and is in this respect similar to the fundamental mode in the case $s = 0$. This similarity masks the above-mentioned discontinuity in the transition between fundamental modes on arc cathodes with $s = 0$ and $s = 1$. It is worth noting that this discontinuity remained unnoticed, although the difficulties arising at low currents in calculations of the (pseudo)diffuse mode on wide cathodes with the use of the diffuse mode at $s = 0$ as an initial approximation have been known for many years, and was realized only recently, after similar difficulties have been encountered in the modelling of glow discharge.

The numerical approach to finding steady-state 3D solutions that has been used in the existing literature allows one to find only solutions possessing planar symmetry. A question arises as to whether non-symmetric steady-state 3D solutions exist. 3D solutions that branch off from 1D and 2D solutions indeed possess planar symmetry; however, one cannot exclude the possibility of breaking of this symmetry through a bifurcation. The latter can happen indeed, as shown by the example of the bifurcation $\{3D, 3D\}$ described in section 5.

7. Conclusions

Bifurcations of modes of current transfer to cathodes of dc gas discharges do occur in numerical modelling, also in apparently simple situations. A failure to recognize and properly analyse a bifurcation may originate difficulties in the modelling and hinder understanding of numerical results and the underlying physics.

All basic types of steady-state bifurcations (fold, transcritical, pitchfork) are encountered in numerical modelling of current transfer to cathodes of dc glow and arc discharges. Dramatic changes in patterns of dc current transfer occur in both glow and arc discharges through perturbed transcritical bifurcations of first- and second-order contact.

Analysis of bifurcations allows one to understand main features of patterns of steady-state modes and their stability. For example, the analysis elucidates the reason why the mode associated with the falling section of the CVC in the classic 1D solution of von Engel and Steenbeck seems not to appear in 2D numerical modelling and the subnormal and normal modes appear instead. A similar effect has been identified in numerical modelling of arc cathodes and explained.

Multiple modes of current transfer to dc discharge cathodes represent a self-organization phenomenon. In spite of physical mechanisms of discharges on cold and hot cathodes being very different, the self-organization fits into the same pattern. However, there are some differences, for example different scenarios of exchange of branches in breaking of transcritical bifurcations of first-order contact. This difference originates in the fact that an absorbing wall locally quenches the glow discharge due to loss of the charged particles caused by diffusion to the wall, while lateral heating of an arc cathode increases the temperature of the cathode edge and thus locally enhances the discharge. Another difference is that the fundamental mode of a glow discharge in a tube with an absorbing wall manifests a normal spot, while the fundamental mode on an arc cathode with a current- and energy-collecting lateral surface is characterized by modest variations of parameters along the front surface of the cathode and is in this respect similar to the diffuse mode. This

difference stems from the essentially different aspect ratio. A further difference is that modes with regular patterns of two or more spots are not observed on arc cathodes, but have been observed in glow discharges [5–10]. This difference remains to be explained.

Acknowledgments

The work was performed within activities of the project PTDC/FIS/68609/2006 Cathode spots in high-pressure dc gas discharges: self-organization phenomena of FCT, POCI 2010 and FEDER and of the project Centro de Ciências Matemáticas of FCT, POCTI-219 and FEDER. P G C Almeida and M J Faria appreciate financial support from FCT through grants SFRH/BD/30598/2006 and SFRH/BD/35883/2007.

Appendix A. Bifurcations in systems with one degree of freedom

The bifurcation theory is not a tool of everyday use in the gas discharge physics, therefore a brief summary of relevant information seems to be in place. There is extensive literature on the subject, e.g. [47–50]. On the other hand, the concepts needed for this work are quite natural and may be summarized in a concise and self-sufficient form.

Appendix A.1. Bifurcations in systems governed by a single parameter

As far as bifurcations are concerned, most systems with a large and even infinite number of degrees of freedom, such as continuum systems, are similar to simple systems with one or two degrees of freedom. (This may be viewed as a consequence of the centre manifold theorem; e.g. [47–50].) Of interest for this work are bifurcations in systems with one degree of freedom. Let us consider a system with one degree of freedom governed by a single parameter μ and described by the equation

$$\frac{\mathrm{d}x}{\mathrm{d}t} = F, \tag{7}$$

where t is time (the independent variable), x is the dependent variable and F is a known function of μ and x, $F = F(\mu, x)$. The simplest forms of the function F that produce bifurcations are the following:

$$F = \mu - x^2, \tag{8}$$

$$F = \mu x - x^2, \tag{9}$$

$$F = \mu x \pm x^3. \tag{10}$$

The steady-state (equilibrium) solutions of differential equation (7) are designated x_0 and governed by algebraic equation $F(\mu, x_0) = 0$. The steady-state solutions for functions F given by equations (8)–(10), are, respectively

$$x_0^{(1)} = -\sqrt{\mu}, \qquad x_0^{(2)} = \sqrt{\mu}, \tag{11}$$

$$x_0^{(1)} = 0, \qquad x_0^{(2)} = \mu, \tag{12}$$

$$x_0^{(1)} = 0, \qquad x_0^{(2)} = -\sqrt{\mp\mu}, \qquad x_0^{(3)} = \sqrt{\mp\mu}. \tag{13}$$

These solutions are shown in figures 14(*a*)–(*d*).

In all the cases, the origin $\mu = x_0 = 0$ belongs to more than one solution. This phenomenon is called branching, or bifurcation, of solutions; the point $\mu = x_0 = 0$ is called the bifurcation point; and figures 14(*a*)–(*d*) are called bifurcation diagrams. The bifurcation described by equation (11) and shown in figure 14(*a*) is called fold or saddle–node. Note that functions $x_0^{(1)}(\mu)$ and $x_0^{(2)}(\mu)$ given by equation (11) may be viewed not as separate solutions but rather as branches of a single solution, which at $\mu = 0$ reaches a boundary of its existence region, $\mu \geqslant 0$, and turns back. This is why points of fold bifurcations are also called turning points.

The bifurcation described by equation (12) and shown in figure 14(*b*) is called transcritical. It may be viewed as an intersection of two solutions existing on both sides of the bifurcation point (i.e. at both positive and negative μ).

The bifurcations described by equation (13) and shown in figures 14(*c*) and (*d*) are called pitchfork bifurcations. The function $F(\mu, x)$ given by equation (10) is odd with respect to x. In such cases, equation (7) is invariant with respect to the transformation of inversion $x \to -x$. Therefore, if such equation admits a solution $x(t)$, then $-x(t)$ is a solution as well. Such equations always admit a trivial solution, which is symmetric with respect to transformation $x \to -x$; non-trivial solutions can appear only in pairs and are related by this transformation. Indeed, the set of solutions given by equation (13) includes the trivial solution $x_0^{(1)}$ and two non-symmetric solutions $x_0^{(2)}$ and $x_0^{(3)}$, being $x_0^{(2)} = -x_0^{(3)}$. Thus, the bifurcations described by equation (13) and shown in figures 14(*c*) and (*d*) represent branching of a pair of non-symmetric solutions that exists at either $\mu \geqslant 0$ or $\mu \leqslant 0$ from a symmetric solution that exists on both sides of the bifurcation point, and may be viewed as breaking of symmetry.

The three bifurcations considered above are quite common and treated in all textbooks. It is appropriate for the purpose of this work to consider also a less common bifurcation which represents a special case of transcritical bifurcation and is introduced by a function F slightly different from (9): μ is replaced with μ^2 and, for convenience, the sign of the right-hand side is changed, i.e.

$$F = x^2 - \mu^2 x. \tag{14}$$

There are two steady-state solutions for this function,

$$x_0^{(1)} = 0, \qquad x_0^{(2)} = \mu^2, \tag{15}$$

which are shown in figure 14(*e*). The bifurcation is transcritical, similar to the one described by equation (12) and shown in figure 14(*b*). While the two solutions described by equation (12) and shown in figure 14(*b*) cross, i.e. have different first derivatives at the bifurcation point, the two solutions described by equation (15) are tangent at the bifurcation point. This bifurcation will be referred to as transcritical bifurcation of second-order contact. For consistency, the bifurcation described by equation (12) and shown in figure 14(*b*) is referred to in this work as transcritical bifurcation of first-order contact.

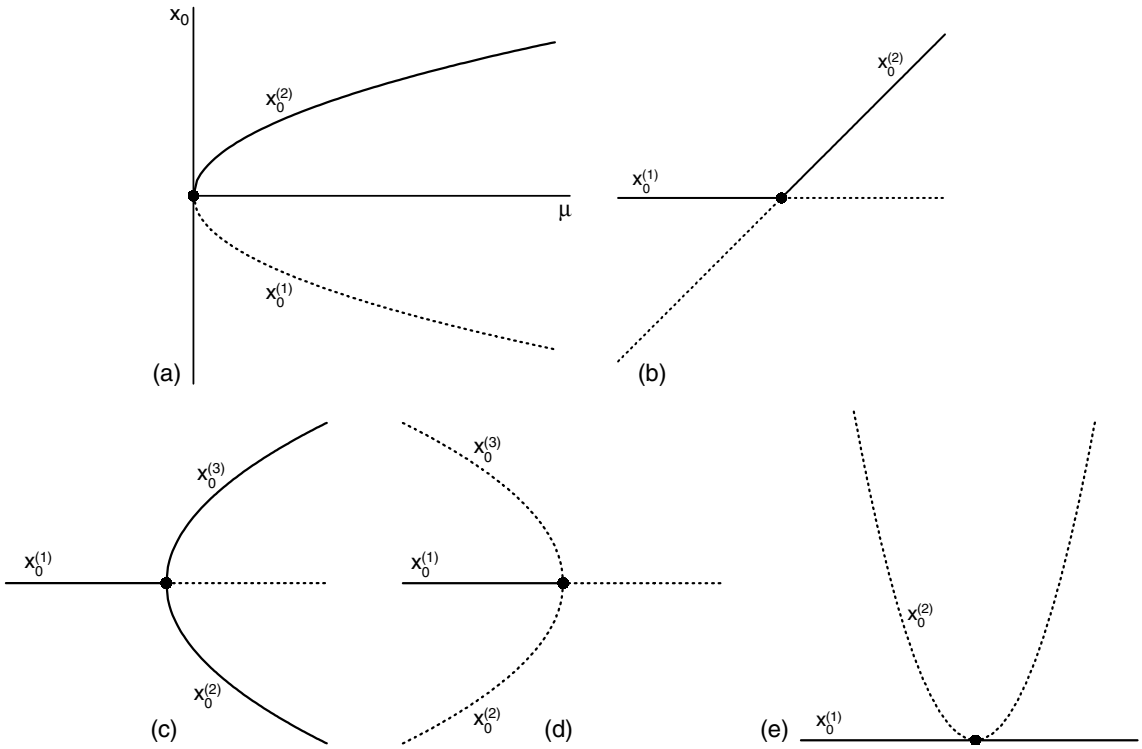

Figure 14. Bifurcation diagrams of steady states in single-parameter systems with one degree of freedom. The origin $\mu = x_0 = 0$ is marked by a circle, axes μ and x_0 in figures (*b*)–(*e*) are the same as in (*a*). Solid: stable sections of steady-state solutions; dotted: unstable sections. (*a*) Fold bifurcation, equation (11). (*b*) Transcritical bifurcation of first-order contact, equation (12). (*c*) Supercritical pitchfork bifurcation, equation (13) with the lower sign. (*d*) Subcritical pitchfork bifurcation, equation (13) with the upper sign. (*e*) Transcritical bifurcation of second-order contact, equation (15).

Appendix A.2. Stability of bifurcating steady-state solutions

Changes in stability of steady-state solutions frequently occur at bifurcation points. In the framework of the conventional procedure of linear stability analysis, a solution of equation (7) is sought as the sum of a steady-state solution and a small perturbation with the exponential time dependence: $x(t) = x_0 + x_1 e^{\lambda t}$, where x_1 is an infinitesimal constant and λ is the growth increment of the perturbation. Substituting this expression into equation (7), expanding the right-hand side in powers of x_1, and retaining only the leading term, one finds

$$\lambda = \frac{\partial F}{\partial x}\left[\mu, x_0\left(\mu\right)\right]. \tag{16}$$

Using this result, one finds that the increments of growth of perturbations of the steady-state solutions $x_0^{(1)}$ and $x_0^{(2)}$ given by equation (11) are, respectively,

$$\lambda^{(1)} = 2\sqrt{\mu}, \qquad \lambda^{(2)} = -2\sqrt{\mu}. \tag{17}$$

It follows that solutions $x_0^{(1)}$ and $x_0^{(2)}$ are unstable and, respectively, stable in the whole region of their existence (which is $\mu \geqslant 0$) except the point $\mu = 0$. $\lambda^{(1)} = \lambda^{(2)} = 0$ at $\mu = 0$, i.e. the solutions are neutrally stable at the fold bifurcation point. In fact, the latter is true for any bifurcation: a bifurcation at the point $\mu = 0$ means that the equation $F(\mu, x_0) = 0$ has multiple roots at small μ, which requires that $\frac{\partial F}{\partial x}(0, 0) = 0$. The above conclusions on stability are illustrated by figure 14(*a*).

Figure 14(*a*) represents an example of a scenario of fold bifurcation, which is conventional in the bifurcation theory. It is convenient for the purpose of this work to mention also the other scenarios, which are obtained by reflection of figure 14(*a*) with respect to the x_0-axis (the second scenario), or with respect to the μ-axis (the third scenario), or with respect to both x_0- and μ-axes (the fourth scenario). Note that these scenarios correspond to replacing equation (8) with, respectively, $F = -x^2 - \mu$, or $F = x^2 - \mu$, or $F = x^2 + \mu$.

The increments of growth of perturbations of solutions (12) are, respectively,

$$\lambda^{(1)} = \mu, \qquad \lambda^{(2)} = -\mu. \tag{18}$$

It follows that solutions $x_0^{(1)}$ and $x_0^{(2)}$ are stable and, respectively, unstable at $\mu < 0$ and vice versa at $\mu > 0$ as shown in figure 14(*b*). One can say that the bifurcating solutions exchange stability at the point of transcritical bifurcation of first-order contact.

The increments of growth of perturbations of solutions (15) are, respectively,

$$\lambda^{(1)} = -\mu^2, \qquad \lambda^{(2)} = \mu^2. \tag{19}$$

It follows that solutions $x_0^{(1)}$ and $x_0^{(2)}$ are stable and, respectively, unstable at all $\mu \neq 0$. In other words, the bifurcating solutions do not change stability at the point of transcritical bifurcation of second-order contact as shown in figure 14(*e*).

The increments of growth of perturbations of solutions given by equations (13) are, respectively,

$$\lambda^{(1)} = \mu, \qquad \lambda^{(2)} = \lambda^{(3)} = -2\mu. \tag{20}$$

The solution $x_0^{(1)}$ is stable at $\mu < 0$ and unstable $\mu > 0$. In other words, the solution $x_0^{(1)}$ changes its stability at the bifurcation point. In the case depicted in figure 14(*c*), which corresponds to the lower sign in equations (10) and (13), both solutions $x_0^{(2)}$ and $x_0^{(3)}$ are stable in the whole region of their existence (except the point $\mu = 0$). In the case depicted in figure 14(*d*), which corresponds to the upper sign, both solutions are unstable. In other words, if the pair of bifurcating solutions branches off into the region where $x_0^{(1)}$ is unstable, then both bifurcating solutions are stable; figure 14(*c*). Pitchfork bifurcations of this type are said to be supercritical. If the pair of bifurcating solutions branches off into the region where the solution $x_0^{(1)}$ is stable, then both bifurcating solutions are unstable (figure 14(*d*)); a subcritical pitchfork bifurcation.

Appendix A.3. Perturbations of transcritical bifurcations in systems governed by two parameters

It is necessary for the purposes of this work to consider also transcritical bifurcations of first- and second-order contact in systems governed by two parameters. Let us introduce a new parameter δ and replace expression (9) with $F = \mu x - x^2 - \delta$ and (14) with $F = x^2 - \mu^2 x + \delta$. Then roots of the equation $F(\mu, x_0) = 0$ are

$$x_0^{(3)} = \tfrac{1}{2}(\mu - \sqrt{\mu^2 - 4\delta}), \qquad x_0^{(4)} = \tfrac{1}{2}(\mu + \sqrt{\mu^2 - 4\delta}) \tag{21}$$

and, respectively,

$$x_0^{(3)} = \tfrac{1}{2}(\mu^2 - \sqrt{\mu^4 - 4\delta}), \qquad x_0^{(4)} = \tfrac{1}{2}(\mu^2 + \sqrt{\mu^4 - 4\delta}). \tag{22}$$

The case $\delta = 0$ was studied in appendix A.1 and a transcritical bifurcation of first-order contact (equation (12) and figure 14(*b*)) or second-order contact (equation (15) and figure 14(*e*)) occurs in this case. Note that the solutions in (15) may be obtained by setting $\delta = 0$ in equation (22), but equation (21) with $\delta = 0$ assumes the form $x_0^{(3)} = \mu$, $x_0^{(4)} = 0$ at $\mu \leqslant 0$ and $x_0^{(3)} = 0$, $x_0^{(4)} = \mu$ at $\mu \geqslant 0$. In other words, the dependences $x_0^{(3)}(\mu)$ and $x_0^{(4)}(\mu)$ given by equation (21) become non-smooth in the case $\delta = 0$ (the first derivative becomes discontinuous), which is why it is natural to use equation (12) in this case.

In the case $\delta < 0$, there are two solutions, one described by the dependence $x_0^{(3)}(\mu)$ and the other by $x_0^{(4)}(\mu)$. These solutions do not have any point in common, i.e. are isolated: the bifurcation is broken. Each of these solutions exists on both sides of the bifurcation point, i.e. at both positive and negative μ. In the case $\delta > 0$, there are two isolated solutions as well, one at negative μ and the other at positive μ. Each of the new solutions comprises two branches separated by a turning point, one branch being described by the dependence $x_0^{(3)}(\mu)$ and the other by $x_0^{(4)}(\mu)$. The above-discussed solutions are schematically shown in figures 15(*a*) and 15(*b*).

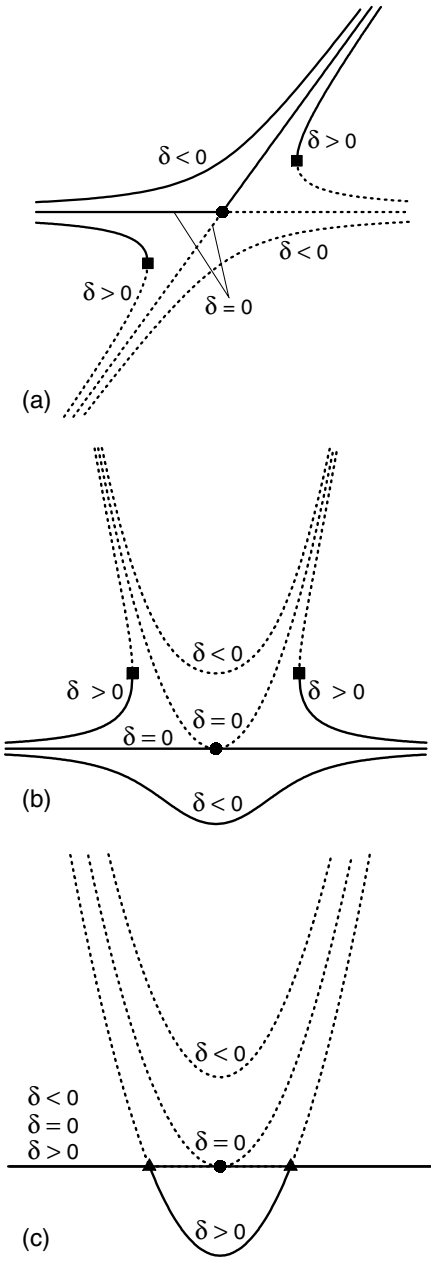

Figure 15. Diagrams of perturbed transcritical bifurcations in two-parameter systems with one degree of freedom. The origin $\mu = x_0 = 0$ is marked by a circle, axes μ and x_0 are the same as in figure 14(*a*). Solid: stable sections of steady-state solutions; dotted: unstable sections. (*a*) Transcritical bifurcation of first order contact, equation (21). (*b*) Transcritical bifurcation of second-order contact, equation (22). (*c*) Transcritical bifurcation of second-order contact, equation (23).

Thus, a perturbation represented by a deviation of δ from zero destroys the bifurcation and causes the bifurcating solutions to be broken into two isolated solutions. Such perturbations are called imperfections.

The stability of each one of the steady-state solutions at $\delta \neq 0$ may be worked out as before (in particular, equation (16) applies) and is illustrated in figures 15(*a*) and (*b*). Regardless

of sign of δ, steady states described by the dependence $x_0^{(3)}$ are unstable and states described by the dependence $x_0^{(4)}$ are stable in the case of the perturbed transcritical bifurcation of first-order contact; vice versa in the case of the perturbed transcritical bifurcation of second-order contact.

The above suggests three possible scenarios of changes in topology of steady-state solutions. The first scenario occurs in the passage from $\delta = 0$ to $\delta > 0$ and represents breaking of the bifurcating solutions $x_0^{(1)}$ and $x_0^{(2)}$ into two isolated solutions formed by joining of branches that exist on the same side of the bifurcation point (i.e. the section of solution $x_0^{(1)}$ in the range $\mu < 0$ joins the section of solution $x_0^{(2)}$ in the same range, the section of $x_0^{(1)}$ in the range $\mu > 0$ joins the section of $x_0^{(2)}$ in the same range). Each one of the new solutions manifests a turning point at which a change in stability occurs according to one of the above-described scenarios of the fold bifurcation.

The second scenario occurs in the passage from $\delta = 0$ to $\delta < 0$ in the case of transcritical bifurcation of first-order contact. This scenario again represents breaking of the bifurcating solutions $x_0^{(1)}$ and $x_0^{(2)}$ with exchange of branches, however in this case the isolated solutions are formed by joining of branches that exist on the opposite sides of the bifurcation point. Each one of the new solutions exists on both sides of the bifurcation point, one of these solutions is stable and the other unstable. Note that no change in topology occurs in the passage from $\delta = 0$ to $\delta < 0$ in the case of transcritical bifurcation of second-order contact: the bifurcating solutions separate without exchange of branches or changes in stability.

The third scenario occurs in the passage from $\delta < 0$ to $\delta > 0$ or vice versa: two isolated solutions approach each other, enter in contact, i.e. a bifurcation occurs, exchange branches and then two isolated solutions appear once again. If the change occurs through a perturbed transcritical bifurcation of first-order contact, then each of the two solutions develops a vertex (i.e. a discontinuity of the first derivative) immediately before entering in contact, and each of the two appearing solutions also possesses a vertex immediately after the separation. If the change occurs through a perturbed transcritical bifurcations of second-order contact, then both solutions remain smooth before entering in contact, and each of the two appearing solutions possesses a cusp immediately after the separation (or vice versa: a cusp before entering in contact and smooth solutions after the separation). Therefore, smooth solutions can change their topology through transcritical bifurcations of second- (or higher) order contact but not first-order contact.

It is convenient for the purpose of this work to consider also another perturbation of transcritical bifurcation of second-order contact which is introduced by replacing expression (14) with $F = x^2 - \mu^2 x + \delta x$. Steady-state solutions of equation (7) read as

$$x_0^{(3)} = 0, \qquad x_0^{(4)} = \mu^2 - \delta. \tag{23}$$

These solutions are schematically shown in figure 15(*c*). Similar to figure 15(*b*), there is a transcritical bifurcation of second-order contact in the case $\delta = 0$ and there are two isolated solutions in the case $\delta < 0$. There are two bifurcations of first-order contact in the case $\delta > 0$ (rather than two isolated solutions as in figure 15(*b*)); the corresponding points are marked by triangles. Note that in the case $\delta > 0$ the section of solution $x_0^{(3)}$ between the bifurcation points is unstable, which, however, cannot be shown on the graph.

This suggests one more possible scenario of changes in topology of steady-state solutions: two smooth isolated solutions approach each other, enter in second-order contact at one point and remain in first-order contact at two points (or vice versa).

References

[1] Raizer Y P 1991 *Gas Discharge Physics* (Berlin: Springer)
[2] http://www.arc_cathode.uma.pt
[3] Kolobov V I and Fiala A 1994 *Phys. Rev.* E **50** 3018–32
[4] Arslanbekov R R and Kolobov V I 2003 *J. Phys. D: Appl. Phys.* **36** 2986–94
[5] Schoenbach K H, Moselhy M and Shi W 2004 *Plasma Sources Sci. Technol.* **13** 177–85
[6] Moselhy M and Schoenbach K H 2004 *J. Appl. Phys.* **95** 1642–9
[7] Takano N and Schoenbach K H 2006 *Plasma Sources Sci. Technol.* **15** S109–17
[8] Arkhipenko V I, Callegari T, Pitchford L, Safronau Y A and Simonchik L V 2007 *Proc. 28th ICPIG (Prague, Czech Republic, July 2007)* ed J Schmidt *et al* (Prague: Institute of Plasma Physics AS CR) ISBN 978-80-87026-01-4 pp 907–10
[9] Lee B J, Rahaman H, Frank K, Mares L and Biborosch D L 2007 *Proc. 28th ICPIG (Prague, Czech Republic, July 2007)* ed J Schmidt *et al* (Prague: Institute of Plasma Physics AS CR) ISBN 978-80-87026-01-4 pp 900–2
[10] Zhu W, Takano N, Schoenbach K H, Guru D, McLaren J, Heberlein J, May R and Cooper J R 2007 *J. Phys. D: Appl. Phys.* **40** 3896–906
[11] Thouret W, Weizel W and Günther P 1951 *Z. Phys.* **130** 621–31
[12] Olsen H N 1963 *J. Quant. Spectrosc. Radiat. Transfer* **3** 305–33
[13] Haidar J 1995 *J. Phys. D: Appl. Phys.* **28** 2494–504
[14] Reiche J, Könemann F, Mende W and Kock M 2001 *J. Phys. D: Appl. Phys.* **34** 3177–84
[15] Lichtenberg S, Nandelstädt D, Dabringhausen L, Redwitz M, Luhmann J and Mentel J 2002 *J. Phys. D: Appl. Phys.* **35** 1648–56
[16] Hartmann T, Günther K, Lichtenberg S, Nandelstädt D, Dabringhausen L, Redwitz M and Mentel J 2002 *J. Phys. D: Appl. Phys.* **35** 1657–67
[17] Mitrofanov N K and Shkol'nik S M 2007 *Tech. Phys.* **52** 711–20
[18] Kühn G and Kock M 2007 *Phys. Rev.* E **75** 016406
[19] Benilov M S, Cunha M D and Faria M J 2008 *IEEE Trans. Plasma Sci.* **36** 1034–5
[20] Benilov M S, Cunha M D and Faria M J 2009 *J. Phys. D: Appl. Phys.* **42** 145205
[21] Bötticher R and Bötticher W 2000 *J. Phys. D: Appl.Phys.* **33** 367–74
[22] Coulombe S 2000 *Bull. Amer. Phys. Soc.* **45** 18 (*53rd Gaseous Electronics Conference* (Houston, TX, October 2000))
[23] Krücken T 2001 *Proc. 9th Int. Symp. on the Science and Technology of Light Sources (Cornell University, Ithaca, NY, August 2001)* ed R S Bergman (Ithaca, NY: Cornell University Press) pp 267–8
[24] Benilov M S and Cunha M D 2002 *J. Phys. D: Appl. Phys.* **35** 1736–50

[25] Benilov M S and Cunha M D 2003 *J. Phys. D: Appl. Phys.* **36** 603–14
[26] Dabringhausen L, Langenscheidt O, Lichtenberg S, Redwitz M and Mentel J 2005 *J. Phys. D: Appl. Phys.* **38** 3128–42
[27] Luijks G M J F, Nijdam S and v Esveld H 2005 *J. Phys. D: Appl. Phys.* **38** 3163–9
[28] Benilov M S, Carpaij M and Cunha M D 2006 *J. Phys. D: Appl. Phys.* **39** 2124–34
[29] Scharf F H, Langenscheidt O and Mentel J 2007 *Proc. 28th ICPIG (Prague, Czech Republic, July 2007)* ed J Schmidt *et al* (Prague: Institute of Plasma Physics AS CR) ISBN 978-80-87026-01-4 pp 1252–5
[30] Lenef A L 2008 *J. Phys. D: Appl. Phys.* **41** 144003
[31] Benilov M S 2008 *J. Phys. D: Appl. Phys.* **41** 144001
[32] Almeida P G C and Benilov M S 2008 *Proc. European COMSOL Conf. (Hannover, Germany 4–6 November 2008)* http://cds.comsol.com/access/dl/papers/ 5253/Almeida.pdf
[33] Almeida P G C, Benilov M S and Faria M J 2009 *Plasma Sources Sci. Technol.* submitted
[34] Kim H C, Iza F, Yang S S, Radmilovic-Radjenovic M and Lee J K 2005 *J. Phys. D: Appl. Phys.* **38** R283–R301
[35] Biondi M A and Chanin L M 1954 *Phys. Rev.* **94** 910–6
[36] Pitchford L C, Boeuf J P and Morgan W L 1998 Boltzmann simulation software and database http://www.siglo-kinema.com/bolsig.htm
[37] Meunier J, Belenguer P and Boeuf J P 1995 *J. Appl. Phys.* **78** 731–745
[38] Fridman A and Kennedy L A 2004 *Plasma Physics and Engineering* (New York: Taylor and Francis)
[39] Benilov M S, Cunha M D and Naidis G V 2005 *Plasma Sources Sci. Technol.* **14** 517–24
[40] Touloukian Y S, Powell R W, Ho C Y and Clemens P G 1970 Thermal conductivity. Metallic elements and alloys *Thermophysical Properties of Matter* vol 1 (New York–Washington: IFI/Plenum)
[41] Benilov M S 2007 *J. Phys. D: Appl. Phys.* **40** 1376–93
[42] Benilov M S and Faria M J 2007 *J. Phys. D: Appl. Phys.* **40** 5083–97
[43] Benilov M S 2008 *Phys. Rev.* E **77** 036408
[44] Benilov M S 1998 *Phys. Rev. E* **58** 6480–94
[45] Benilov M S and Cunha M D 2003 *Phys. Rev.* E **68** 056407
[46] Bötticher R and Bötticher W 2001 *J. Phys. D: Appl. Phys.* **34** 1110–15
[47] Guckenheimer J and Holmes P 1983 Nonlinear oscillations, dynamical systems, and bifurcations of vector fields *Applied Mathematical Sciences* vol 42 (New York: Spinger)
[48] Iooss G and Joseph D D 1990 *Elementary Stability and Bifurcation Theory* 2nd edn (New York: Springer)
[49] Crawford J D 1991 *Rev. Mod. Phys.* **63** 991–1035
[50] Cross M C and Hohenberg P C 1993 *Rev. Mod. Phys.* **65** 851